Cleaved/Associated TLR3 Represents the Primary Form of the Signaling Receptor

Florent Toscano,*,[1] Yann Estornes,*,[1] François Virard,* Alejandra Garcia-Cattaneo,[†] Audrey Pierrot,* Béatrice Vanbervliet,* Marc Bonnin,* Michael J. Ciancanelli,[‡] Shen-Ying Zhang,[‡,§] Kenji Funami,[¶] Tsukasa Seya,[¶] Misako Matsumoto,[¶] Jean-Jacques Pin,[‖] Jean-Laurent Casanova,[‡,§,#] Toufic Renno,* and Serge Lebecque*

TLR3 belongs to the family of intracellular TLRs that recognize nucleic acids. Endolysosomal localization and cleavage of intracellular TLRs play pivotal roles in signaling and represent fail-safe mechanisms to prevent self-nucleic acid recognition. Indeed, cleavage by cathepsins is required for native TLR3 to signal in response to dsRNA. Using novel Abs generated against TLR3, we show that the conserved loop exposed in LRR12 is the single cleavage site that lies between the two dsRNA binding sites required for TLR3 dimerization and signaling. Accordingly, we found that the cleavage does not dissociate the C- and N-terminal fragments, but it generates a very stable "cleaved/associated" TLR3 present in endolysosomes that recognizes dsRNA and signals. Moreover, comparison of wild-type, noncleavable, and C-terminal–only mutants of TLR3 demonstrates that efficient signaling requires cleavage of the LRR12 loop but not dissociation of the fragments. Thus, the proteolytic cleavage of TLR3 appears to fulfill function(s) other than separating the two fragments to generate a functional receptor. *The Journal of Immunology*, **2013, 190: 764–773.**

Toll-like receptors belong to a family of pattern recognition receptors that sense the presence of pathogens and trigger a protective innate immune response (1). These germline-encoded type I integral membrane glycoproteins bind their ligands through their extracellular domain (ECD), which is composed of 19–25 leucine-rich repeats (LRRs) (2). In contrast with other members of the family that primarily recognize molecular patterns specific for nonself invaders, TLR3, TLR7, and TLR9 recognize nucleic acids originating from microbes, as well as from the host. Several fail-safe mechanisms prevent self-polynucleotide recognition and subsequent autoimmune disorders (3). Ligands must be recognized by cell surface receptor(s) (4) that mediate their internalization before encountering the corresponding TLR exclusively in the acidic endolysosomal compartment from which signal transduction can be initiated (5). Delivery of intracellular TLRs to the endocytic compartments is also tightly regulated by the chaperone Unc93b1 (6, 7). Finally, processing by pH-dependent lysosomal proteases is an additional checkpoint for controlling TLR9 activation (8–10).

Although several studies on intracellular TLRs have been based on TLR9 trafficking and processing, less is known about TLR3. TLR3 appears to be dedicated to the recognition of dsRNA (11), and it plays a central role in the defense against HSV-1 infection in the CNS in humans (12–15). Although endogenous mRNA can activate TLR3 in vitro (16), its involvement in the autoimmune response has not been demonstrated. It was shown that TLR3 dimerization is needed for dsRNA binding and signaling (17). Moreover, analysis of the crystal structure (18, 19) and mutagenesis (18, 20, 21) of TLR3 ECD revealed that dsRNA binding requires interaction of the negatively charged ribose backbone of dsRNA with residues of TLR3 dimers located in LRR1 and LRR3, as well as with a second region formed by LRR19–LRR21 that becomes positively charged in the mildly acidified endolysosomal compartment. Therefore, the requirement for cleavage of the ECD for TLR3 signaling (9, 10, 22) raises an intriguing issue with regard to how endogenous TLR3 is processed and which forms of the receptor recognize dsRNA. In this study, we generated and used novel mAbs directed against TLR3 ECD and mutant forms of TLR3 to demonstrate that cleavage of the LRR12 loop, but not separation of the two fragments, is required for signaling.

Materials and Methods

Cell culture and reagents

HEK293 and HEK293-TLR3-hemagglutinin (HA) cells (InvivoGen) were grown in DMEM medium (Invitrogen) supplemented with 10% FBS and penicillin/streptomycin. Human bronchial epithelial cell line BEAS-2B (Sigma) was cultured in LHC-9 medium (Invitrogen) in bovine collagen

*Centre de Recherche en Cancérologie de Lyon, INSERM Unité Mixte de Recherche 1052/Centre National de la Recherche Scientifique 5286, Centre Léon Bérard, 69008 Lyon, France; [†]Institut Curie, INSERM U932, 75005 Paris, France; [‡]St. Giles Laboratory of Human Genetics of Infectious Diseases, Rockefeller Branch, The Rockefeller University, New York, NY 10065; [§]Laboratory of Human Genetics of Infectious Diseases, Necker Branch, INSERM U980, University Paris Descartes, Paris 75015, France; [¶]Department of Microbiology and Immunology, Graduate School of Medicine, Hokkaido University, Kita-ku, Sapporo 060-8638, Japan; [‖]DENDRITICS SAS, Bioparc Laennec, 69008 Lyon, France; and [#]Pediatric Immunology-Hematology Unit, Necker Hospital for Sick Children, Paris 75015, France

[1]F.T. and Y.E. contributed equally to this work.

Received for publication August 21, 2012. Accepted for publication November 15, 2012.

This work was supported by Cancéropôle Lyon-Auvergne-Rhône-Alpes.

F.T., Y.E., F.V., A.G.-C., M.J.C., S.-Y.Z., T.S., M.M., T.R., and S.L. designed the experiments. F.T., Y.E., F.V., A.G.-C., A.P., B.V., S.-Y.Z., M.J.C., M.B., K.F., and J.-J.P. performed experiments and analyzed data. F.T., Y.E., F.V., J.-L.C., T.R., and S.L. wrote the manuscript, with all authors providing detailed comments and suggestions. S.L. directed the project.

Address correspondence and reprint requests to Prof. Serge Lebecque, Centre de Recherche en Cancérologie de Lyon, INSERM Unité Mixte de Recherche 1052/Centre National de la Recherche Scientifique 5286, Centre Léon Bérard, 28 rue Laennec, 69008 Lyon, France. E-mail address: serge.lebecque@univ-lyon1.fr

The online version of this article contains supplemental material.

Abbreviations used in this article: DC, dendritic cell; ECD, extracellular domain; EEA, early endosome Ag; EndoH, endoglycosidase H; ER, endoplasmic reticulum; FL, full length; HA, hemagglutinin; HMW, high molecular weight; LMW, low molecular weight; LRR, leucine-rich repeat; mDC, monocyte-derived dendritic cell; NSCLC, non-small cell lung cancer; PNGase, peptide:*N*-glycosidase F; Poly(A:U), polyadenylic-polyuridylic acid; Poly(I:C), polyinosinic-polycytidylic acid; siRNA, small interfering RNA; WT, wild-type.

www.jimmunol.org/cgi/doi/10.4049/jimmunol.1202173

type I (Invitrogen) and fibronectin (Sigma)-coated dishes. $CD14^+$ monocytes were purified from peripheral blood of healthy donors: PBMCs were isolated from human peripheral blood by standard density-gradient centrifugation on Pancoll (PAN Biotech) and then mononuclear cells were separated from PBLs on a 50% Percoll solution (GE Healthcare). Monocytes were enriched by one step of adherence and differentiated in immature dendritic cells (DCs) in complete RPMI 1640 medium supplemented with 200 ng/ml human GM-CSF (kind gift of Schering-Plough) and 50 ng/ml human rIL-4 (R&D Systems) for 6 d. NCI-H292 and NCI-H1703 non-small cell lung cancer (NSCLC) cell lines (American Type Culture Collection) were grown in RPMI 1640 medium (Invitrogen) supplemented with 10% FBS (Sigma), HEPES, NaPy, 100 U/ml penicillin/streptomycin, and 2 mM glutamine. THP1 and U937 cell lines were grown in RPMI 1640 medium (Invitrogen) supplemented with 10% FBS and 100 U/ml penicillin/streptomycin. IFN-α was from Schering-Plough. Z-FA-fmk, chloroquine, tunicamycin, and cycloheximide were from Sigma. Polyinosinic-polycytidylic acid [Poly(I:C)]-high molecular weight (HMW) and Poly(I:C)-low molecular weight (LMW) were purchased from InvivoGen. polyadenylic-polyuridylic acid [Poly(A:U)] was from Innate Pharma. Mouse monoclonal IgG1 anti-actin Ab was from MP Biomedicals. Anti-mouse TLR3 Ab T3.7C3 was a gift from Nadège Goutagny (Centre de Recherche sur le Cancer de Lyon, Lyon, France). HRP-conjugated donkey anti-mouse secondary Ab was from Jackson ImmunoResearch.

TLR3.2 and TLR3.3 Ab preparation and purification

BALB/C mice were immunized with recombinant human TLR3 ECD (R&D Systems) by three i.p. injections of the immunogen in the presence of Freund's adjuvant and a final i.v. boost, 3 d before spleen isolation. Splenic cells were fused with the SP20 myeloma cell line in the presence of polyethylene glycol. Hybridoma supernatants were screened by immunofluorescent staining of pUNO-hTLR3-HA and pUNO-hTLR3-V5 transiently transfected 293T cells with Exgen 500 (Euromedex) and fixed with acetone. Only clones recognizing both transfected cells were selected.

Western blotting

Cells were lysed in cold lysis buffer (20 mM Tris-HCl [pH 7.4], 150 mM NaCl, 0.2% Nonidet P-40, supplemented with 1 mM orthovanadate, 10 mM NaF, and a protease inhibitor mixture; Sigma) for 25 min on ice. Cell lysates were cleared by centrifugation (13,000 × *g* for 10 min at 4°C), and protein concentration was determined using the Bradford assay (Bio-Rad). Protein lysates were denatured or not in Laemmli buffer containing 1% SDS and 5 mM DTT and heated to 95°C for 5 min. For peptide:*N*-glycosidase F (PNGase)/endoglycosidase H (EndoH) digestions, lysates were treated as recommended by the manufacturer (New England BioLabs). Proteins were resolved on SDS-polyacrylamide gels and transferred onto polyvinylidene difluoride membranes by electroblotting, and nonspecific binding sites were blocked using TBS containing 0.1% Tween-20 and 5% (w/v) dry milk. After incubation with the appropriate secondary Abs conjugated to HRP, blots were revealed using ECL (GE Healthcare) or SuperSignal (Thermo Scientific) reagents. For reimmunoprecipitation experiments, anti-TLR3 or anti-HA immunoprecipitates were eluted with preheated lysis buffer containing 1% SDS and 5 mM DTT; 20% of each sample was resolved by SDS-PAGE, and the remaining 80% was diluted 10-fold in lysis buffer and then reimmunoprecipitated with TLR3.2 or anti-HA Ab, resolved by SDS-PAGE, and analyzed with either TLR3.2 or TLR3.3 Ab.

Immunofluorescence

Cells were washed with PBS, fixed with 4% formaldehyde for 10 min at room temperature, and washed three times with PBS. Cells were then blocked using Image-iT FX signal enhancer (Life Technologies) for 30 min at room temperature and washed once with PBS. Thereafter, each washing step was done using TBS. Cells were incubated for 1 h at room temperature with TLR3.1, anti-HA, anti-calreticulin, early endosome Ag (EEA)1, or Lamp1 (Abcam) primary Abs. After washing three times, cells were incubated for 30 min at room temperature with secondary Abs (goat anti-mouse–Alexa Fluor 488 and goat anti-rabbit–Alexa Fluor 555 or Alexa Fluor 633; Life Technologies). Cells were washed again 3 min each. Cover slips were air-dried and then mounted using ProLong Gold antifade reagent with DAPI (Life Technologies). Images were acquired using a confocal microscope (Zeiss Axiovert 100 M LSM510) with a 1.4 NA Plan-Apochromat 63× oil-immersion lens. Image noise was reduced using a Despeckle Fiji filter.

Cytokines measurement

The supernatant from NCI-H292 and NCI-H1703 cells, cultured or not with 100 μg/ml Poly(I:C) for 24 h, was assayed for IL-6, IP-10, and RANTES using a MILLIPLEX MAP kit (Millipore) on a Luminex Bio-Plex 200 System Analyzer (Bio-Rad). The supernatant from monocyte-derived DCs (mDCs), cultured or not with 100 μg/ml Poly(I:C) for 24 h, was assayed for IL-6, IP-10, TNF-α, and IFN-λ using a Quantikine ELISA test (R&D Systems), as described by the manufacturer.

DNA cloning

Preparation of the LRR1-11 and 13-21 deletion mutants was described previously (23). For the TLR3-Ins12-HA mutant, mutagenesis was performed using the QuikChange XL Site-Directed Mutagenesis Kit (Stratagene) and primer pairs containing deletion of 24 nucleotides: 5′-CTGAATTTGAAACG-GTCTTTTACTCTCCCCAAGATTGATGATTTTTCT-3′ (forward) and 5′-AGAAAAATCATCAATCTTGGGGAGAGTAAAAGACCGTTTCAAA-TTCAG-3′ (reverse). Ten nanograms of plasmid DNA and 125 ng of primers were used, according to the manufacturer's instructions. Two colonies from each library were sequenced.

For the TLR3-$Cter_{356}$-HA mutant, LRR deletion mutants of TLR3 (A_{22}–K_{356}) were generated by PCR with Phusion (Finnzyme), using the appropriate primers: 5′-TGTTTGGAGCACCTTAACATGGAAG-3′ (forward) and 5′-GGTGGAGGATGCACACAGCATCCCA-3′ (reverse). PCR was performed with the following cycling conditions: 10 s at 98°C, 2 min at 72°C for 25 cycles. The PCR product was treated with DpnI to digest the template DNA, phosphorylated with T4 PNK (New England BioLabs), and ligated using a DNA Ligation kit (New England BioLabs). Deletion constructs were sequenced. TLR3-$Cter_{346}$ was provided by P. Bénaroch (Curie Institute, Paris, France).

RNA interference

Synthetic TRIF (L-012833-00-0005) and control nonsilencing (D-001810-03-20) small interfering RNAs (siRNAs) were from Dharmacon. TLR3 Stealth RNAi siRNA (TLR3HSS110816) was from Invitrogen. siRNAs mix was prepared in Opti-MEM medium (Invitrogen), and cells in suspension were transfected using HiPerFect reagent (QIAGEN), as described by the manufacturer. The final siRNA concentrations were 25 nM. Transfected cells were seeded in 6-well plates or 96-well white plates (Greiner) and incubated for 24 h. Medium was replaced with fresh complete medium, and cells were incubated for 48 h before Poly(I:C) treatment.

Generation of ISRE– and NF-κB–luciferase reporter cell lines

HEK293, NCI-H292, and NCI-H1703 cells were transduced with luciferase ISRE- or NF-κB–reporter lentiviruses (SABiosciences), according to the manufacturer's recommendations, and transduced cells were selected with puromycin.

Reporter luciferase assays

Cells were seeded in white 96-well plates (10,000 cells/well); 24 h later they were treated with 10 μg/ml poly(I:C) in 50 μl medium for 4 or 6 h, depending on the cell line. Then, 50 μl Steady-Glo reactive (Promega) was added to each well before reading luminescence with a Tecan Infinite 200 microplate reader using i-control software (Tecan).

Transient expression in HEK293 cells

Cells were seeded in 100-mm dishes to reach ~70% confluence on the day of transfection. Cells were transfected with pUNO, TLR3–wild-type (WT)-HA, TLR3-Ins12-HA, TLR3-$Cter_{356}$-HA, or TLR3-$Cter_{346}$-HA by incubating 8 μl Lipofectamine 2000 (Invitrogen) with 8 μg plasmid in 6 ml Opti-MEM medium for 5 h; subsequently, Opti-MEM was replaced by fresh medium. Twenty-four hours after transfection, cells were trypsinized and seeded in 96-well white plates and 6-well plates and incubated for 24 h.

Stable transfections

P2.1 cells were transfected with pUNO-hTLR3 vectors, which contain WT TLR3 cDNA, TLR3-Ins12 mutant, or TLR3-Cter356 mutant cDNA, or with an empty mock vector, in the presence of Lipofectamine Reagent (Invitrogen) and PLUS Reagent (Invitrogen), as described by the manufacturer. Stable transfectants were selected with medium containing blasticidin (5 μg/ml; Invitrogen). The presence of TLR3 was confirmed by Western blotting.

Determination of mRNA levels by RT-quantitative PCR

Total RNA was extracted from P2.1 cells. RNA was reverse-transcribed using Oligo-deoxy-thymidine. To determine mRNA levels for IL-29, quantitative PCR was performed with Assays-on-Demand probe/primer combinations and 2× universal reaction mixture in an ABI Prism 7700 Sequence Detection System (all from Applied Biosystems). The β-glucuronidase (GUS) gene was used for normalization. Results are expressed according to the ΔCt method, as described by the manufacturer.

Coimmunoprecipitation

Cells were cultured in 150-mm dishes, collected, washed in PBS, and lysed in 750 μl cold lysis buffer (20 mM Tris-HCl [pH 7.4], 150 mM NaCl, 0.2% Nonidet P-40, supplemented with 1 mM orthovanadate, 10 mM NaF, and a protease inhibitor mixture; Sigma) for 25 min on ice. Cell lysates were cleared by centrifugation (13,000 × *g* for 10 min at 4°C). Lysates were precleared with 50 μl Sepharose-6B (Sigma) for 1 h at 4°C and then immunoprecipitated overnight at 4°C with 5 μg mouse anti-TLR3.2, anti-TLR3.3, or control IgG1 Ab (R&D Systems) and the following day in the presence of 20 μl protein G–Sepharose for 3 h at 4°C. Beads were recovered by centrifugation, and immunoprecipitates were washed extensively with lysis buffer and eluted with Laemmli buffer containing 1% SDS and 5 mM DTT and heated to 95°C for 10 min.

TLR3 ECD modeling

The MacPyMOL software (DeLano Scientific) was used to generate the 3D representation of the TLR3 structure shown on Figs. 1C and 5A (PDB:1ZIW).

Statistical analysis

Statistical significance was determined using the Student *t* test.

Results

Profiling endogenous TLR3 expression

To analyze the biology of endogenous TLR3, we generated three new mAbs (designated as TLR3.1, TLR3.2, and TLR3.3) raised against the ECD of the receptor. First, the Abs were validated using HEK293 cells stably expressing TLR3 tagged with a C-terminal HA epitope (HEK293-TLR3-HA). In this model, Western blots probed with anti-HA, TLR3.2, and TLR3.3 Abs revealed an ~130 kDa band corresponding to the expected molecular mass of highly glycosylated TLR3 (Fig. 1A) (24). The stronger signal observed with TLR3.2 suggested that this Ab has a higher affinity for TLR3 than does TLR3.3. In addition, anti-HA and TLR3.2 Abs stained a second band at ~72 kDa similar to the C-terminal fragment of TLR3 observed after cleavage by cathepsin. In addition, TLR3.3 Ab detected a third band (Fig. 1A) not recognized by anti-HA mAb and with a size ~60 kDa that could represent the N-terminal fragment of cleaved TLR3. TLR3.1 Ab did not detect TLR3 by Western blot, but it showed the same staining by immunofluorescence as observed with anti-HA Ab (Fig. 1B, Supplemental Fig. 1A). To unequivocally identify the different bands revealed by TLR3.2 and TLR3.3 Abs on Western blot, we mapped the recognized epitopes using 20 single LRR-deleted forms of the ECD of TLR3 (LRR1–11 and LRR13–21) (23). Fig. 1C establishes that TLR3.2 Ab recognizes an epitope present in LRR20, whereas TLR3.3 binds to an epitope formed by residues present in LRR7 and LRR8. We next verified whether similar expression profiles could be observed in human cells of different origins and wondered how treatment with IFN-α, which is known to upregulate the expression of TLR3 (25), would modify this pattern. We determined TLR3 expression by immunoblot of lysates from mDCs (Fig. 1D), from human monocytic cell lines U937 and THP1 (Supplemental Fig. 1B, 1C), and from human bronchial epithelial cells transformed by SV40-T Ag (BEAS-2B; Supplemental Fig. 1D) or derived from NSCLC (NCI-H292 and NCI-H1703; Fig. 1E). The three forms of TLR3 (130, 72, and 60 kDa) were present in every lysate with the exception of THP1, which did not appear to express TLR3 (Supplemental Fig. 1B) or respond to Poly(I:C) (Supplemental Fig. 1E). Resting MRC-5 cells were also devoid of TLR3, but kinetic analysis showed that IFN-α treatment led first to the detection of the high molecular mass bands (~130 and ~135 kDa) of TLR3, followed by an increase in the intensity of the lower ~72-kDa molecular mass band detected by TLR3.2 mAb (Fig. 1F), suggesting that the former might

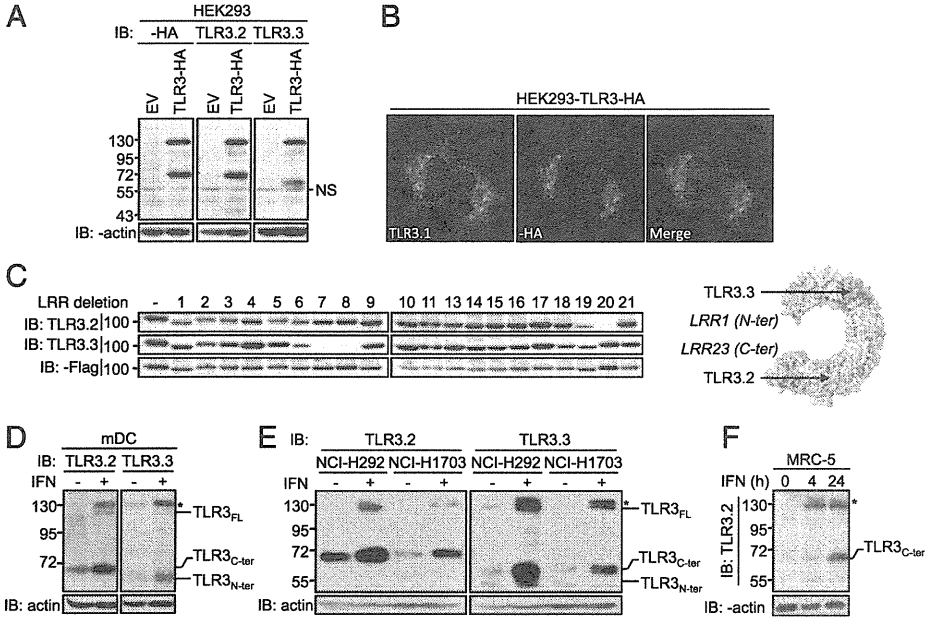

FIGURE 1. Profiling endogenous TLR3 expression. (**A**) Immunoblot analysis of HEK293 cells stably expressing an empty vector (EV) or TLR3-HA; lysates were analyzed with monoclonal anti-HA, TLR3.2, TLR3.3, and anti-actin Abs. (**B**) Immunofluorescence of HEK293 cells stably expressing TLR3-HA; cells were stained with anti-HA or TLR3.1 Abs, followed by DAPI nuclear staining (blue). Original magnification ×63. (**C**) *Left panel*, Epitope mapping of TLR3.2 and TLR3.3 Abs on HEK293 cells stably transfected with TLR3-HA WT (−) or TLR3-HA mutants carrying LRR deletions (1–11 and 13–21, as indicated). Lysates were analyzed with monoclonal TLR3.2, TLR3.3, and anti-Flag Abs, as indicated. *Right panel*, Schematic representation of epitopes recognized by TLR3.2 and TLR3.3 Abs on TLR3 ECD. (**D**) Immunoblot analysis of mDCs treated (+) or not (−) for 18 h with IFN-α (1000 IU/ml); lysates were analyzed with TLR3.2, TLR3.3, and anti-actin Abs. (**E**) Immunoblot analysis of NCI-H292 and NCI-H1703 cells treated (+) or not (−) for 18 h with IFN-α (1000 IU/ml); lysates were analyzed with TLR3.2, TLR3.3, and anti-actin Abs. (**F**) Immunoblot analysis of MRC-5 cells treated (+) or not (−) for the indicated times with IFN-α (1000 IU/ml); lysates were analyzed with TLR3.2 and anti-actin Abs. Values in (A) and (C)–(F) represent molecular mass (kDa). All data are representative of at least three independent experiments. NS, Nonspecific band.

represent the precursors of the latter. In other cell lines, the absolute and relative intensities of the three bands varied depending on the origin of the cells, the Ab used, and the treatment with IFN-α. However, under basal conditions, all cells primarily expressed the 72 and 60 kDa TLR3 forms. Treatment with IFN-α increased the intensity of the three bands and allowed the detection of a higher molecular mass form ~135 kDa in mDCs and in the four cell lines analyzed (asterisk in Fig. 1D–F and Supplemental Fig. 1D). In conclusion, our data suggest that human TLR3 is spontaneously cleaved into a C-terminal fragment ~72 kDa recognized by TLR3.2 and a C-terminal fragment ~60 kDa recognized by TLR3.3, and the relative abundance of cleaved versus uncleaved TLR3 appears to vary with the cell under consideration.

TLR3 ECD cleavage by cathepsins generates two remarkably stable fragments

To further explore the processing of endogenous TLR3 and its functional consequences, we selected the NCI-H292 and NCI-H1703 NSCLC cell lines, which triggered an innate immune response when stimulated with Poly(I:C), as indicated by cytokine secretion (Supplemental Fig. 2A) and by activation of ISRE-dependent luciferase reporter genes (Supplemental Fig. 2B). We ascertained that this response was mediated exclusively by TLR3 by showing its strict dependence on TRIF, the only known adaptor for TLR3 (Supplemental Fig. 2B). We started analyzing the effects of the cathepsin inhibitor Z-FA-fmk on the expression of the different forms of TLR3. Following Z-FA-fmk treatment, the 130 kDa band became more intense with time, whereas the 72 and 60 kDa bands gradually disappeared in both NCI-H292 and NCI-H1703 cells (Fig. 2A, Supplemental Fig. 2C, respectively), as well as in HEK293-TLR3-HA cells (Fig. 2B). These results confirm that cathepsins are necessary for TLR3 cleavage in epithelial cells (22). In NCI-H292 cells, the accumulation of full-length TLR3 was observed as early as 120 min after the addition of Z-FA-fmk (Fig. 2C), whereas in the three cell lines both C-terminal ($TLR3_{C\text{-}ter}$) and N-terminal ($TLR3_{N\text{-}ter}$) TLR3 fragments disappeared with an apparent $t_{1/2}$ >24 h (Fig. 2A, 2B, Supplemental Fig. 2C). Of note, Z-FA-fmk induces a shift of TLR3 full-length ($TLR3_{FL}$) from 130 kDa to 135 kDa ($TLR3_{FL+}$) in both NSCLC cell lines, which is more visible after prolonged gel migration (Fig. 2D). This $TLR3_{FL+}$ could represent the fully glycosylated form of TLR3 leaving the post-Golgi cisternae and not cleaved yet. Published data with regard to the effects of cathepsin inhibitors on TLR3 signaling seem contradictory (8, 9). In this study, we observed that ISRE- and NF-κB–dependent responses to Poly(I:C) were not modified after prolonged treatment with Z-FA-fmk in NCI-H292 cells (Supplemental Fig. 2D), whereas they were significantly, but not completely, suppressed in NCI-H1703 cells (Supplemental Fig. 2E). However, considering the much higher level of TLR3 expression in resting NCI-H292 cells than in NCI-H1703 cells (Fig. 1E), the amounts of $TLR3_{C\text{-}ter}$ detected in NCI-H292 cells after 72 h of treatment with Z-FA-fmk was still comparable to the basal level in NCI-H1703 cells. Therefore, these results suggest that cleaved TLR3 is important for signaling, although uncleaved TLR3 might still transduce some signal. Importantly, Z-FA-fmk treatment blocked TLR3 cleavage and Poly(I:C)-induced cytokine secretion in mDCs (Fig. 2E, 2F) and TR3 signaling in macrophages U937 cells (Fig. 2G, Supplemental Fig. 2F), whereas the response to TNF-α was unaffected. Like with Z-FA-fmk treatment, exposure to the lysosomotropic weak base chloroquine, which prevents cathepsin activity, led to the accumulation of $TLR3_{FL+}$ within 3 h and to the reciprocal disappearance of the two TLR3 fragments in NCI-H292 (Fig. 2H) and NCI-H1703 (Supplemental Fig. 2G) cells after 48 h. The same results were obtained with the specific inhibitor of vacuolar H^+ ATPase Bafilomycin (data not shown). Furthermore, short-term blockade of de novo protein synthesis with cycloheximide confirmed the relative high stability of endogenous $TLR3_{C\text{-}ter}$ (apparent $t_{1/2}$ > 24 h) (Fig. 2I, 2J) compared with $TLR3_{FL}$ (apparent $t_{1/2}$ < 4 h). Despite a weaker signal, a half-life similar to $TLR3_{C\text{-}ter}$ was estimated for $TLR3_{N\text{-}ter}$ (Fig. 2H, Supplemental Fig. 2G). Altogether, our data indicate that, in resting cells, TLR3 is actively transcribed and rapidly cleaved by cathepsins upon its transfer in endolysosomes into two highly stable proteolytic fragments, in agreement with a very recent report (26).

TLR3 transits steadily through the Golgi before being cleaved in the endolysosomal compartments

Although TLR3, like other intracellular TLRs, depends on the chaperone protein Unc93b1 for proper trafficking, it is unclear whether its transfer to the endolysosomes occurs constitutively or in response to its ligand. Using TLR3.1 Ab, we observed by immunofluorescence microscopy that TLR3 colocalizes extensively with Lamp1 (a lysosome marker) but not with EEA1 (an early endosome marker) (Fig. 3A, Supplemental Fig. 3) in resting epithelial cells and that the level of colocalization remained unchanged after stimulation with dsRNA (Supplemental Fig. 3). We next addressed the trafficking of TLR3 by analyzing the N-glycosylation status of the protein, which represents ~35% of its total mass (24). After treatments of cell lysates with PNGase, which removes all N-glycans, $TLR3_{FL}$ and $TLR3_{FL+}$ shifted from 130 and 135 kDa, respectively, to 95 kDa (Fig. 3B, 3C), corresponding to the expected molecular mass of nonglycosylated neosynthesized $TLR3_{FL}$ (904 aa). The $TLR3_{C\text{-}ter}$ band shifted from 72 to 50 kDa, indicating that both cleaved and noncleaved TLR3 are glycosylated. Treatment with EndoH, an endoglycosidase that cleaves N-glycans before their further modification in the Golgi apparatus, indicates that noncleaved $TLR3_{FL}$ is EndoH sensitive, whereas $TLR3_{FL+}$ and $TLR3_{C\text{-}ter}$ are partially EndoH resistant. This was similar to the presence of hybrid glycans on TLR9 even after trafficking through the Golgi (27). Cell treatment with tunicamycin, a de novo *N*-glycosylation inhibitor, caused the rapid fading of $TLR3_{FL}$ (apparent $t_{1/2}$ < 8 h) and the appearance of a band at ~95 kDa representing neosynthesized nonglycosylated full-length TLR3 (Fig. 3D, 3E). Altogether, our data indicate that $TLR3_{FL}$ corresponds to the small amounts of TLR3 present in the endoplasmic reticulum (ER), which is steadily translocated to the Golgi in resting cells, converted into fully glycosylated $TLR3_{FL+}$, and exported to the endosomes/lysosomes, where it is rapidly cleaved.

The endolysosomal pool of cleaved TLR3 is sufficient for signaling

To determine which forms of endogenous TLR3 are functional, we started using specific siRNA and took advantage of the prolonged stability of cleaved fragments versus $TLR3_{FL}$. We observed that 24 and 48 h after transfection, $TLR3_{FL}$ had completely disappeared, whereas the two cleavage fragments were still abundant (Fig. 4A, Supplemental Fig. 4A). Under these conditions, the Poly(I:C)-induced ISRE-dependent response was not reduced (Fig. 4B), suggesting that the uncleaved $TLR3_{FL}$ does not contribute significantly to downstream signaling, probably because of its weak expression compared with the cleaved fragments from the beginning of the experiment. Indeed, ISRE activation faded away gradually with time as the presence of cleaved TLR3 decreased (Fig. 4A, 4B). Similar results were obtained with a NF-κB–dependent reporter gene (Supplemental Fig. 4B). These data show that cleaved TLR3 can signal in the absence of uncleaved $TLR3_{FL}$ and may even represent the predominant signaling form of the receptor.

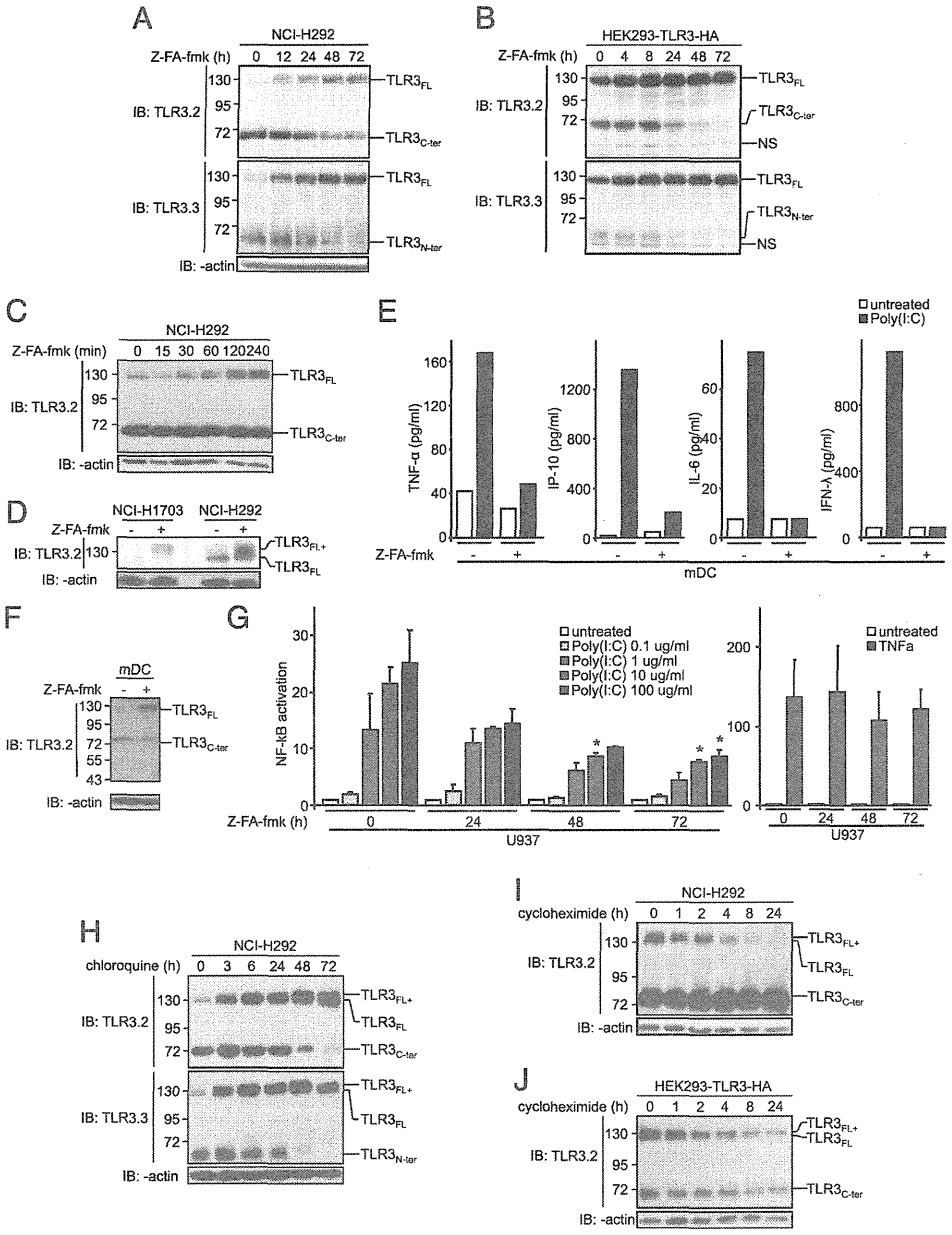

FIGURE 2. Cleavage by cathepsins generates two TLR3 stable fragments. (**A**) Immunoblot analysis of NCI-H292 cells treated for the indicated times with Z-FA-fmk (20 μM) renewed every 24 h. Lysates were analyzed with TLR3.2, TLR3.3, and anti-actin Abs. (**B**) Immunoblot analysis of HEK293-TLR3-HA cells treated for the indicated times with Z-FA-fmk (20 μM) renewed every 24 h. Lysates were analyzed with TLR3.2 and TLR3.3 Abs. (**C**) Immunoblot analysis of NCI-H292 cells treated for the indicated times with Z-FA-fmk (20 μM). Lysates were analyzed with TLR3.2 and anti-actin Abs. (**D**) Immunoblot analysis of NCI-H292 and NCI-H1703 cells treated for 24 h with Z-FA-fmk (20 μM). Lysates were analyzed with TLR3.2 and anti-actin Abs. (**E**) Cytokine production in mDCs that were pretreated for 48 h with Z-FA-fmk and then treated with Poly(I:C) (10 μg/ml) for 24 h. (**F**) Immunoblot analysis of mDCs that were treated or not for 72 h with Z-FA-fmk (20 μM); lysates were analyzed with TLR3.2 and anti-actin Abs. (**G**) NF-κB reporter assay in U937 cells that were pretreated for the indicated times with Z-FA-fmk (20 μM), renewed every 24 h, and then treated with Poly(I:C) at the indicated concentrations (*left panel*) or with TNF-α (50 ng/ml) (*right panel*) for 4 h. (**H**) Immunoblot analysis of NCI-H292 cells treated for the indicated times with chloroquine (1 μg/ml). Lysates were analyzed with TLR3.2, TLR3.3, and anti-actin Abs. (**I**) Immunoblot analysis of NCI-H292 cells treated for the indicated times with cycloheximide (1.5 μg/ml). Lysates were analyzed with TLR3.2 and anti-actin Abs. (**J**) Immunoblot analysis of HEK293-TLR3-HA cells treated for the indicated times with cycloheximide (1.5 μg/ml). Lysates were analyzed with TLR3.2 and anti-actin Abs. Values represent molecular mass (kDa). Data are mean (G) or representative (A–F, H–J) of at least three independent experiments. $*p < 0.05$, untreated cells versus Z-FA-fmk–treated cells.

The N- and C-terminal fragments of TLR3 ECD are needed for efficient signaling

To definitely establish the functionality of uncleaved versus cleaved TLR3, we expressed three mutants of TLR3 in HEK293 cells. Given the apparent molecular mass of deglycosylated $TLR3_{C\text{-}ter}$ and $TLR3_{FL}$ (50 and 95 kDa, respectively; Fig. 3B, 3C), the highly conserved insertion within LRR12, which protrudes on the glycosylation-free side of LRR12 (residues 335–342) (28–31), was a likely site for proteolysis. Thus, the first mutant lacked the entire LRR12 insertion (TLR3-Ins12-HA), whereas the two others represented the C-terminal fragment starting just at the end of the LRR12 insertion (aa 346: TLR3-$Cter_{346}$-HA), as established and

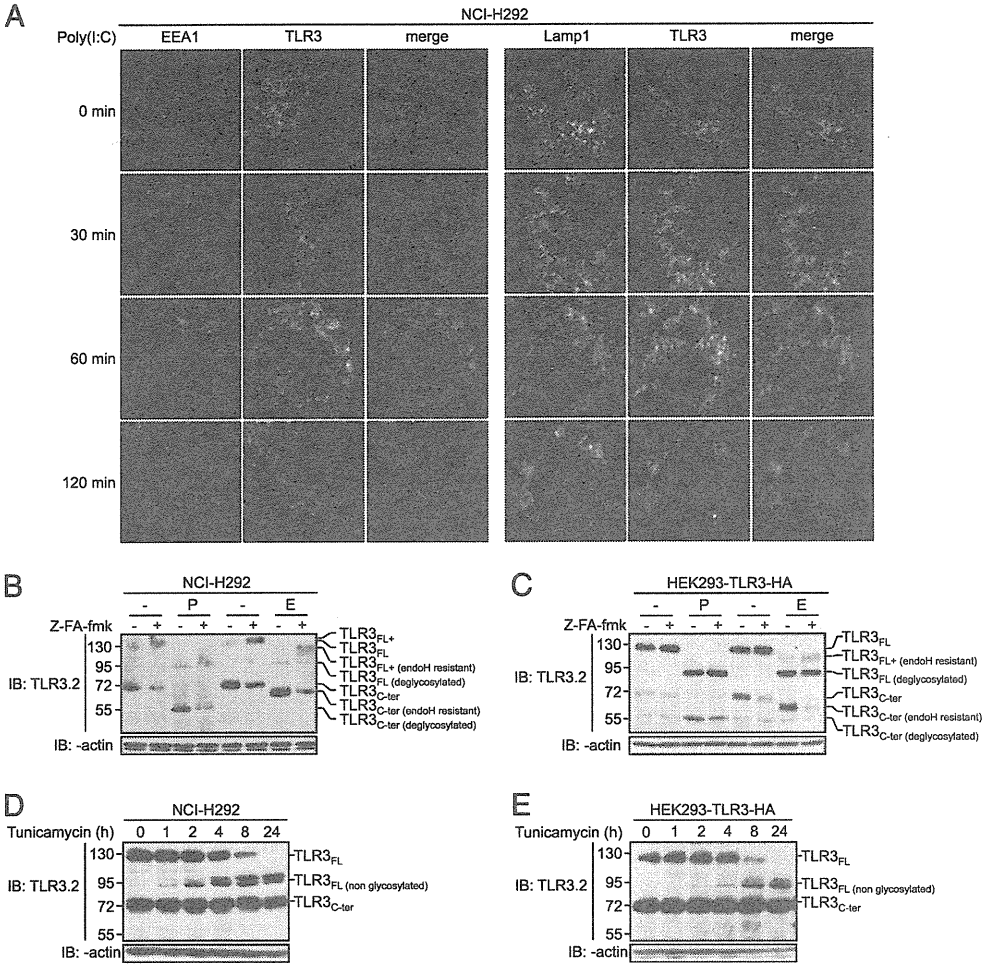

FIGURE 3. TLR3 transits through the Golgi before being cleaved in the endolysosomal compartments. (**A**) Immunofluorescence of NCI-H292 cells treated for the indicated times with Poly(I:C) (10 μg/ml) and then stained with EEA1 or Lamp1, and TLR3.1 Abs, followed by DAPI nuclear staining (blue). Original magnification ×63. (**B**) Immunoblot analysis of NCI-H292 cells that were treated or not with Z-FA-fmk (20 μM) for 24 h. Lysates were left untreated (−) or were treated (+) with PNGase (P) or EndoH (E) and then analyzed with TLR3.2 and anti-actin Abs. (**C**) Immunoblot analysis of HEK293-TLR3-HA cells that were treated or not with Z-FA-fmk (20 μM) for 24 h. Lysates were left untreated (−) or were treated (+) with PNGase (P) or EndoH (E) and then analyzed with TLR3.2 and anti-actin Abs. (**D**) Immunoblot analysis of NCI-H292 cells that were treated for the indicated times with tunicamycin (1 μg/ml). Lysates were analyzed with TLR3.2 and anti-actin Abs. (**E**) Immunoblot analysis of HEK293-TLR3-HA cells that were treated for the indicated times with tunicamycin (1 μg/ml). Lysates were analyzed with TLR3.2 and anti-actin Abs. Values in (B)–(D) represent molecular mass (kDa). Data are representative of at least three independent experiments.

characterized by Garcia-Cattaneo et. al (22), or at the beginning of LRR13 (aa 356: TLR3-Cter$_{356}$-HA) (Fig. 5A). Immunoblots confirmed that all three constructs were expressed at comparable levels in HEK-293T–transfected cells (Fig. 5B), with TLR3-Ins12-HA expressed as a single 130-kDa band, confirming that the LRR12 insertion contains the cleavage site and that TLR3-Ins12-HA is a noncleavable form of the receptor. As expected, lysates from TLR3-Cter$_{356}$-HA– or TLR3-Cter$_{346}$-HA–transfected cells contained a single form ~72 kDa, whose size is consistent with the predicted length of each construct (Fig. 5B). We also observed that treatment with Poly(I:C) did not modify the processing of TLR3 and, particularly, did not induce the cleavage of TLR3-Ins12-HA (Fig. 5B).

When expressed in HEK293 cells, the noncleavable form of the receptor showed the capacity to activate ISRE- and NF-κB–dependent transcription in response to 10 μg/ml of Poly(I:C) (Fig. 5C)

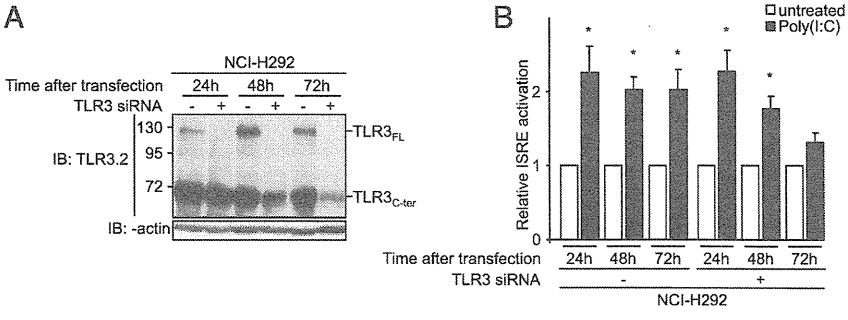

FIGURE 4. Endogenous cleaved TLR3 is sufficient to fully signal. (**A**) Immunoblot analysis of NCI-H292 cells at the indicated times after nonsilencing (−) or TLR3 (+) siRNA transfections (25 μM). Lysates were analyzed with TLR3.2 and anti-actin Abs. (**B**) ISRE reporter assay in NCI-H292 cells at the indicated times after nonsilencing (−) or TLR3 (+) siRNA transfections (25 μM) and treatment without or with Poly(I:C) (10 μg/ml) for 4 h. Data are representative (A) or the mean (B) of three independent experiments. Error bars represent SEM. *$p < 0.05$, untreated cells versus Poly(I:C)-treated cells.

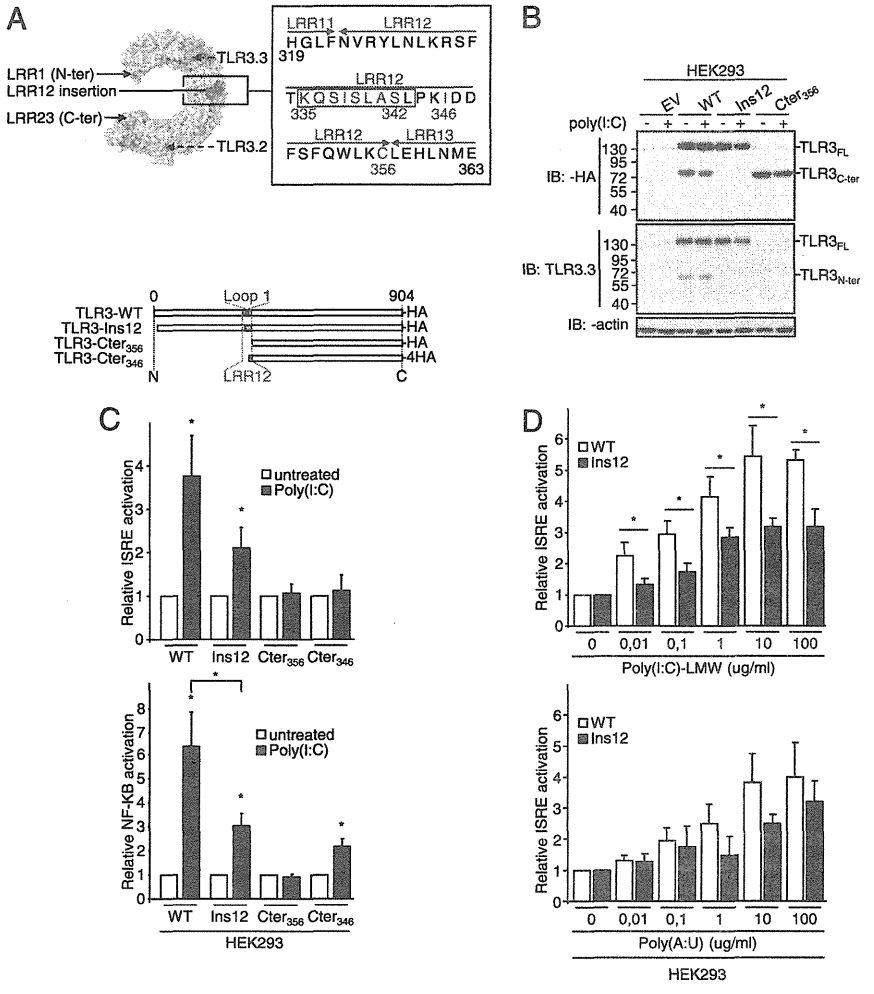

FIGURE 5. Noncleaved TLR3 can signal but the isolated C-terminal TLR3 fragment cannot. (**A**) *Upper panel*, Model of the putative location of the cleavage on LRR12 and TLR3 sequence with starting points of TLR3-$Cter_{356}$ and TLR3-$Cter_{346}$ mutants and deleted sequence (aa 335–342) of TLR3-Ins12 (in red). Blue framework: LRR12 loop1. *Lower panel*, Schematic representation of TLR3 mutants. (**B**) Immunoblot analysis of HEK293 cells transfected with empty vector (EV), TLR3-WT-HA (WT), TLR3-Ins12-HA (Ins12), or TLR3-$Cter_{356}$-HA ($Cter_{356}$) and then treated without (−) or with (+) Poly(I:C) (10 μg/ml) for 4 h. Lysates were analyzed with anti-HA, TLR3.3, and anti-actin Abs. Values represent molecular mass (kDa). (**C**) ISRE (*upper panel*) and NF-KB (*lower panel*) reporter assay in HEK293 cells transfected with TLR3-WT-HA, TLR3-Ins12-HA, TLR3-$Cter_{356}$-HA ($Cter_{356}$), or TLR3-$Cter_{346}$-HA ($Cter_{346}$), and then treated without (white) or with (black) Poly(I:C) (10 μg/ml) for 6 h. (**E**) ISRE reporter assay in HEK293 cells transfected with TLR3-WT-HA or TLR3-Ins12-HA and then treated with the indicated concentrations of Poly(I:C)-LMW or Poly(A:U) for 6 h. Data are representative (B) or the mean (C, D) of at least three independent experiments. Error bars (C, D) represent SEM. *$p < 0.05$, untreated versus Poly(I:C)-treated cells or response of TLR3-WT versus mutant TLR3.

but with significantly reduced efficiency for NF-κB compared with WT TLR3. In contrast, TLR3-$Cter_{356}$-HA was unable to activate either pathway, and TLR3-$Cter_{346}$-HA triggered a weak NF-κB response but no ISRE-dependent response. We next compared the levels of ISRE-dependent transcription in response to increasing concentrations of either LMW Poly(I:C) or Poly(A:U). The dose responses showed that HEK293 cells transfected with WT TLR3 were also significantly more sensitive to LMW Poly(I:C) but not to Poly(A:U) (Fig. 5D). Notably, both C-terminal fragments of the receptor were completely unresponsive to all doses of these two ligands (data not shown). Taken together, these results show that, in agreement with previous reports, uncleaved TLR3 can generate a response to dsRNA (30), whereas the isolated C-terminal fragment triggers only a weak signal (26).

The N- and C-terminal fragments of TLR3 remain associated after cleavage

Because cleaved TLR3 was able to signal in the total absence of $TLR3_{FL}$ (Fig. 4A, 4B, Supplemental Fig. 4A, 4B), whereas isolated $TLR3_{C\text{-}ter}$ was almost ineffective (Fig. 5C), we wondered whether the two fragments of TLR3 could remain associated after proteolytic cleavage. Therefore, we compared the profiles of TLR3 on Western blot performed with lysates prepared in nondenaturing (protein lysate neither reduced nor heated) versus denaturing conditions (Fig. 6A–D, Supplemental Fig. 4C). In nondenaturing conditions, we detected the 130 kDa band, whereas bands corresponding to the proteolytic fragments were barely detectable in epithelial NCI-H292 cells (Fig. 6A, Supplemental Fig. 4C), in mDCs (Fig. 6B), as well as in HEK293-TLR3-HA cells (Fig. 6C, 6D). We ensured that nondenaturing conditions did not prevent the migration of TLR3 fragments, because the constructs corresponding to the cleaved $TLR3_{C\text{-}ter}$ fragment ($Cter_{356}$ and $Cter_{346}$) migrated at expected molecular mass (~72 kDa; Fig. 6D). In contrast, when the same lysates were analyzed in denaturing conditions, $TLR3_{C\text{-}ter}$ and $TLR3_{N\text{-}ter}$ became clearly visible (Fig. 6A–D, Supplemental Fig. 4C), thereby revealing the presence of both uncleaved and cleaved/associated TLR3 in cells. Similarly, when nondenatured lysates were immunoblotted after running on a native gel, the same high molecular band was observed, with HEK293 cells expressing either WT or noncleavable TLR3 and with epithelial cells expressing endogenous TLR3 (Supplemental Fig. 4D). In contrast, the $TLR3_{C\text{-}ter}$ mutant migrated on the same gel at a much lower molecular mass. Moreover, nondenaturing conditions showed that Poly(I:C) treatment did not dissociate $TLR3_{C\text{-}ter}$ and $TLR3_{N\text{-}ter}$ (Fig. 6A–C, Supplemental Fig. 4C). To definitely confirm the association of the two cleaved fragments, we performed immunoprecipitation with C-terminal–specific TLR3.2 and N-terminal–specific TLR3.3 Abs and analyzed the precipitates by immunoblot with the two Abs. In all cases, $TLR3_{N\text{-}ter}$ and $TLR3_{C\text{-}ter}$ coimmunoprecipitated both in NCI-H292 cells (Fig. 6E) and HEK293-TLR3-HA cells (Fig. 6F). Lastly, reprecipitation after denaturation of the immunoprecipitates ob-

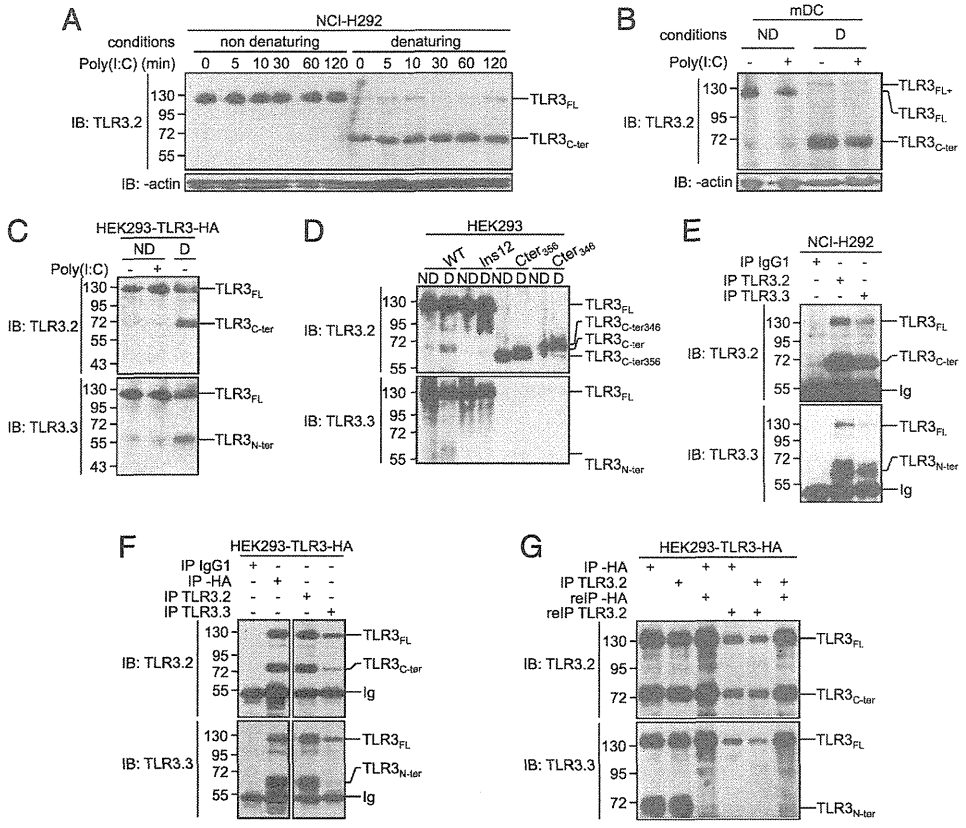

FIGURE 6. The N- and C-terminal fragments of endogenous TLR3 fragments remain associated after cleavage. (**A**) Immunoblot analysis of NCI-H292 cells treated with Poly(I:C) (10 μg/ml) for the indicated times. Lysates were denatured (D) or not (ND) and then analyzed with TLR3.2 and anti-actin Abs. (**B**) Immunoblot analysis of mDCs treated (+) or not (−) with Poly(I:C) (10 μg/ml) for the indicated times. Lysates were denatured (D) or not (ND) and then analyzed with TLR3.2 and anti-actin Abs. (**C**) Immunoblot analysis of HEK293-TLR3-HA cells treated (+) or not (−) with Poly(I:C) (10 μg/ml) for 2 h. Lysates were denatured (D) or not (ND) and then analyzed with TLR3.2 and TLR3.3 Abs. (**D**) Immunoblot analysis of HEK293 cells transfected with TLR3-WT-HA (WT), TLR3-Ins12-HA (Ins12), TLR3-Cter$_{356}$-HA (Cter$_{356}$), or TLR3-Cter$_{346}$-HA (Cter$_{346}$). Lysates were denatured (D) or not (ND) and then analyzed with TLR3.2 and TLR3.3 Abs. (**E**) Immunoblot analysis of NCI-H292 cells. Lysates were immunoprecipitated with IgG1, TLR3.2, or TLR3.3 Abs and analyzed with TLR3.2 and TLR3.3 Abs. (**F**) Immunoblot analysis of HEK293-TLR3-HA cells. Lysates were immunoprecipitated with IgG1, anti-HA, TLR3.2, or TLR3.3 Abs and analyzed with TLR3.2 and TLR3.3 Abs. (**G**) Immunoblot analysis of HEK293-TLR3-HA cells. Lysates were immunoprecipitated with anti-HA or TLR3.2 Abs and then precipitates were reimmunoprecipitated with anti-HA or TLR3.2 Abs and analyzed with TLR3.2 and TLR3.3 Abs. Values represent molecular mass (kDa). Data are representative of at least three independent experiments.

tained with a C-terminal–specific Ab (either TLR3.2 or anti-HA) led to the loss of the N-terminal fragment of TLR3, confirming that the association of the two fragments was through a noncovalent bond (Fig. 6G). Taken together, our data show that the two fragments of TLR3 remain associated after cleavage and that ligand binding does not disrupt this association (Fig. 7). Therefore, the cleaved/associated TLR3 represents the relevant endogenous TLR3 responsible for the majority of immunological functions.

Discussion

Remarkable progress has been made recently in our understanding of the biology of nucleic acid–sensing TLR3, TLR7, and TLR9. Notably, various data now suggest a model in which exogenous nucleotides can be recognized with high sensitivity, whereas self-nucleotide–induced signaling and autoimmunity are prevented (3). Discrimination between nonself- and self-nucleotides appears to be facilitated by several levels of regulation. Recently, cleavage of TLR9 in endolysosomes was shown to be required for generating the C-terminal fragment of the receptor that binds dsDNA with high affinity and signals. Published data indicated that this mechanism might also apply to TLR3 and TLR7 (9, 22). However, our data allow us to propose an alternative model for TLR3 biology (Fig. 7), which reconciles two requisites: the need to restrict dsRNA recognition in endolysosomes (and therefore to expose the receptor to a proteolytic environment) to prevent autoreactivity, as described for other endosomal TLRs, and the requirement of the two ligand binding sites present on the ECD of TLR3—the first near the N terminus and the second close to the transmembrane region—to recognize dsRNA with high avidity. Several aspects of the trafficking and processing of TLR3 diverge from what has been described for other lysosomal TLRs (8, 10).

Building on previous observations, and supported by data that were published after the submission of our manuscript (26), our results allow improvement of our model of TLR3 biology. In contrast to TLR9, which was reported to reside principally in the ER in resting cells (32) and to reach the acidic compartments after stimulation by double-stranded DNA (5–7, 33), TLR3 is continuously exported to the Golgi and accumulates in the endolysosomal compartments where it undergoes a single cleavage by cathepsins, most likely within the short (9 aa) LRR12 external loop; however, the exact cleavage site remains unknown. In contrast, asparagine endopeptidase first cleaves the long (30 aa) LRR14–15 flexible loop of TLR9 that is secondarily trimmed by cathepsins (8–10, 34, 35). Strong conservation of the LRR12 ex-

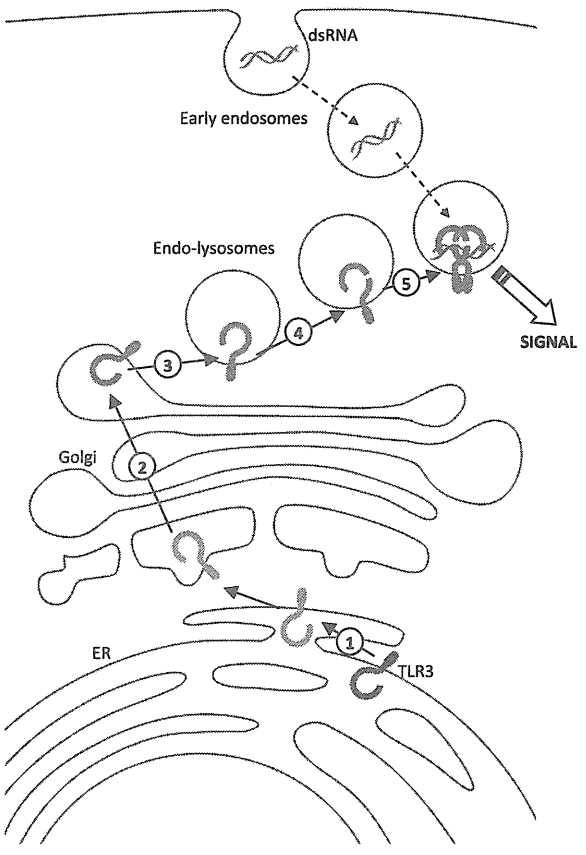

FIGURE 7. Proposed model of TLR3 processing. (**1**) TLR3 is neosynthesized and *N*-glycosylated in the ER. (**2**) Then, it crosses the Golgi apparatus where it is fully glycosylated to become EndoH resistant. TLR3 exits the Golgi to enter the endosome membrane (**3**) where it is cleaved by cathepsins (**4**). The two proteolytic fragments remain associated to fully signal (**5**).

ternal loop (residues 335–343) during mammals' evolution (30) suggests that cleavage is an important step in the biology of TLR3. Remarkably, our data confirm that the two proteolytic fragments of the ECD of TLR3 have prolonged half-lives (26) and demonstrate that they remain associated, suggesting that the noncovalent interactions between the adjacent LRRs known to stabilize the ECD of TLRs (36) have been preserved. Furthermore, the absence of detectable amounts of Golgi-modified $TLR3_{FL+}$ in resting immune and nonimmune cells (Figs. 1A, 1D–F, 3B, 3C) indicates that cleaved/associated TLR3 is the almost exclusive form of the receptor present in endolysosomes, where the encounter with exogenous dsRNA is known to occur (37). The lack of appropriate ligand prevented us from visualizing directly TLR3 bound to dsRNA. However, the physical association of TRIF with $TLR3_{C\text{-}ter}$, but not $TLR3_{FL}$, after activation with Poly(I:C) in NCI-H292 cells (38), combined with the absence of free $TLR3_{C\text{-}ter}$ in those cells, indicates that cleaved/associated TLR3 is the main form of the receptor recognizing Poly(I:C). The single cleavage, without further trimming, may explain why the two long-lived fragments of TLR3 remain associated to bind dsRNA. In contrast, although it was proposed that some TLR9 fragments could remain associated (8, 39), the C-terminal fragment of the receptor is viewed as the major form of the functional receptor, binding agonist CpG oligodesoxynucleotides with high affinity and being able to efficiently recruit the adaptor protein MyD88 (8, 10).

The streamlined transfer to endolysosomes, followed by rapid cleavage, explains why endogenous TLR3 fragments were abundant in resting cells of every type analyzed, whereas $TLR3_{FL}$ was difficult to detect. In contrast, comparable amounts of $TLR3_{FL}$ and TLR3 fragments were observed in HEK293 cells, suggesting an imbalance between the high expression of exogenous TLR3 and the availability of the chaperone protein Unc93b1 in those cells (26). Indeed, exogenous TLR3 was abundant in the ER, whereas endogenous TLR3 was found mostly in the endolysosomes. Moreover, the half-lives of the fragments from transfected TLR3 were shorter compared with endogenous TLR3 (compare Fig. 2B with Fig. 2A). These differences should be kept in mind when studying the biology of endosomal TLRs in HEK293 cells.

TLR3 cleavage could increase or decrease the sensitivity of the receptor and/or modify its specificity for different ligands. Our functional studies reveal that, in TLR3-transfected HEK293 cells, the cleavage increased the sensitivity to HMW and LMW Poly(I:C). The increased sensitivity of cleaved/associated TLR3 remains perplexing. Thus, cleavage could somehow increase the affinity of the ECD for its ligands or ease the conformational change that may occur in the presence of dsRNA (39) and that may facilitate the recruitment of TRIF. In agreement with Qi et al. (26), we observed that $TLR3_{C\text{-}ter}$ by itself was consistently unable to trigger a strong response to dsRNA. A difference in timing (6 versus 18 h) might explain, in part, the variance between those results and recently published data that showed an equal response to Poly(I:C) with either TLR3-WT or $TLR3_{C\text{-}ter}$ (22). Whatsoever the residual activity of $TLR3_{C\text{-}ter}$, its physiological importance is uncertain, because cleaved/associated TLR3 appears to be the predominant form of the endogenous receptor present in the endolysosomes where recognition of dsRNA takes place.

The central role of cleaved/associated TLR3 highlights the importance for dsRNA binding affinity and sensitive signaling of two distinct ligand-binding sites, each present on one proteolytic fragment. Moreover, the increased sensitivity to Poly(I:C) and the remarkable stability of this form of the receptor allows the reconciliation of some apparently discordant results from the literature. Indeed, one group reported the absence of inhibition of TNF production by RAW macrophages treated for 12 h with cathepsin inhibitors and then for 2 h with 100 μg/ml of Poly(I:C) (8), whereas another group showed a strong suppression of TNF production by the same cells in response to 1 μg/ml of Poly(I:C) (9). These different outcomes may be due to differences in the concentration of ligand used, with high concentrations of dsRNA being able to activate the less efficient $TLR3_{FL}$ in these cells. In addition, our data show that 12 h of Z-FA-fmk pretreatment is not sufficient to suppress the expression of TLR3 fragments in NSCLC cells, suggesting that the lack of inhibition by Z-FA-fmk of cells activated with moderate concentrations of Poly(I:C) could have resulted from the persistence of some cleaved/associated TLR3 at the time of stimulation.

In conclusion, TLR3 provides the first example, to our knowledge, of endosomal receptor maturation by cleavage followed by conversion into a functional cleaved/associated form of the protein. Considering that cleavage of WT-TLR3 is necessary for signaling, cleaved/associated TLR3 is the principal (and possibly exclusive) signaling receptor, and noncleavable TLR3 is able to signal, an intriguing conclusion of the present work is that the licensing consequence of TLR3 cleavage for signaling is not the separation of the two fragments. Further studies are required to fully evaluate the structural and functional consequences of TLR3 processing in vitro and in vivo, as well as to determine to what extent some aspects of TLR3 biology might apply to the other endolysosomal TLRs.

Acknowledgments

We thank Olivier Micheau (Bourgogne University, Dijon, France) for critical reading of the manuscript, Philippe Benaroch for reviewing the results and for the plasmid gift, and Sebastian Amigorena for discussions (both at Curie Institute, Paris, France).

Disclosures

The authors have no financial conflicts of interest.

References

1. Kawai, T., and S. Akira. 2011. Toll-like receptors and their crosstalk with other innate receptors in infection and immunity. *Immunity* 34: 637–650.
2. Gay, N. J., and M. Gangloff. 2007. Structure and function of Toll receptors and their ligands. *Annu. Rev. Biochem.* 76: 141–165.
3. Barton, G. M., and J. C. Kagan. 2009. A cell biological view of Toll-like receptor function: regulation through compartmentalization. *Nat. Rev. Immunol.* 9: 535–542.
4. Limmon, G. V., M. Arredouani, K. L. McCann, R. A. Corn Minor, L. Kobzik, and F. Imani. 2008. Scavenger receptor class-A is a novel cell surface receptor for double-stranded RNA. *FASEB J.* 22: 159–167.
5. Barton, G. M., J. C. Kagan, and R. Medzhitov. 2006. Intracellular localization of Toll-like receptor 9 prevents recognition of self DNA but facilitates access to viral DNA. *Nat. Immunol.* 7: 49–56.
6. Tabeta, K., K. Hoebe, E. M. Janssen, X. Du, P. Georgel, K. Crozat, S. Mudd, N. Mann, S. Sovath, J. Goode, et al. 2006. The Unc93b1 mutation 3d disrupts exogenous antigen presentation and signaling via Toll-like receptors 3, 7 and 9. *Nat. Immunol.* 7: 156–164.
7. Kim, Y.-M., M. M. Brinkmann, M.-E. Paquet, and H. L. Ploegh. 2008. UNC93B1 delivers nucleotide-sensing toll-like receptors to endolysosomes. *Nature* 452: 234–238.
8. Park, B., M. M. Brinkmann, E. Spooner, C. C. Lee, Y.-M. Kim, and H. L. Ploegh. 2008. Proteolytic cleavage in an endolysosomal compartment is required for activation of Toll-like receptor 9. *Nat. Immunol.* 9: 1407–1414.
9. Ewald, S. E., A. Engel, J. Lee, M. Wang, M. Bogyo, and G. M. Barton. 2011. Nucleic acid recognition by Toll-like receptors is coupled to stepwise processing by cathepsins and asparagine endopeptidase. *J. Exp. Med.* 208: 643–651.
10. Ewald, S. E., B. L. Lee, L. Lau, K. E. Wickliffe, G.-P. Shi, H. A. Chapman, and G. M. Barton. 2008. The ectodomain of Toll-like receptor 9 is cleaved to generate a functional receptor. *Nature* 456: 658–662.
11. Alexopoulou, L., A. C. Holt, R. Medzhitov, and R. A. Flavell. 2001. Recognition of double-stranded RNA and activation of NF-kappaB by Toll-like receptor 3. *Nature* 413: 732–738.
12. Casrouge, A., S.-Y. Zhang, C. Eidenschenk, E. Jouanguy, A. Puel, K. Yang, A. Alcais, C. Picard, N. Mahfoufi, N. Nicolas, et al. 2006. Herpes simplex virus encephalitis in human UNC-93B deficiency. *Science* 314: 308–312.
13. Zhang, S.-Y., E. Jouanguy, S. Ugolini, A. Smahi, G. Elain, P. Romero, D. Segal, V. Sancho-Shimizu, L. Lorenzo, A. Puel, et al. 2007. TLR3 deficiency in patients with herpes simplex encephalitis. *Science* 317: 1522–1527.
14. Guo, Y., M. Audry, M. Ciancanelli, L. Alsina, J. Azevedo, M. Herman, E. Anguiano, V. Sancho-Shimizu, L. Lorenzo, E. Pauwels, et al. 2011. Herpes simplex virus encephalitis in a patient with complete TLR3 deficiency: TLR3 is otherwise redundant in protective immunity. *J. Exp. Med.* 208: 2083–2098.
15. Matsumoto, M., H. Oshiumi, and T. Seya. 2011. Antiviral responses induced by the TLR3 pathway. *Rev. Med. Virol.* 21: 67–77.
16. Karikó, K., H. Ni, J. Capodici, M. Lamphier, and D. Weissman. 2004. mRNA is an endogenous ligand for Toll-like receptor 3. *J. Biol. Chem.* 279: 12542–12550.
17. Wang, Y., L. Liu, D. R. Davies, and D. M. Segal. 2010. Dimerization of Toll-like receptor 3 (TLR3) is required for ligand binding. *J. Biol. Chem.* 285: 36836–36841.
18. Bell, J. K., J. Askins, P. R. Hall, D. R. Davies, and D. M. Segal. 2006. The dsRNA binding site of human Toll-like receptor 3. *Proc. Natl. Acad. Sci. USA* 103: 8792–8797.
19. Liu, L., I. Botos, Y. Wang, J. N. Leonard, J. Shiloach, D. M. Segal, and D. R. Davies. 2008. Structural basis of toll-like receptor 3 signaling with double-stranded RNA. *Science* 320: 379–381.
20. Fukuda, K., T. Tsujita, M. Matsumoto, T. Seya, H. Sakiyama, F. Nishikawa, S. Nishikawa, and T. Hasegawa. 2006. Analysis of the interaction between human TLR3 ectodomain and nucleic acids. *Nucleic Acids Symp. Ser. (Oxf)* 50: 249–250.
21. Watanabe, T., T. Tokisue, T. Tsujita, M. Matsumoto, T. Seya, S. Nishikawa, T. Hasegawa, and K. Fukuda. 2007. N-terminal binding site in the human toll-like receptor 3 ectodomain. *Nucleic Acids Symp. Ser. (Oxf)* 51: 405–406.
22. Garcia-Cattaneo, A., F. X. Gobert, M. Müller, F. Toscano, M. Flores, A. Lescure, E. Del Nery, and P. Benaroch. 2012. Cleavage of Toll-like receptor 3 by cathepsins B and H is essential for signaling. *Proc. Natl. Acad. Sci. USA* 109: 9053–9058.
23. Takada, E., S. Okahira, M. Sasai, K. Funami, T. Seya, and M. Matsumoto. 2007. C-terminal LRRs of human Toll-like receptor 3 control receptor dimerization and signal transmission. *Mol. Immunol.* 44: 3633–3640.
24. Sun, J., K. E. Duffy, C. T. Ranjith-Kumar, J. Xiong, R. J. Lamb, J. Santos, H. Masarapu, M. Cunningham, A. Holzenburg, R. T. Sarisky, et al. 2006. Structural and functional analyses of the human Toll-like receptor 3. Role of glycosylation. *J. Biol. Chem.* 281: 11144–11151.
25. Kaiser, W. J., J. L. Kaufman, and M. K. Offermann. 2004. IFN-α sensitizes human umbilical vein endothelial cells to apoptosis induced by double-stranded RNA. *J. Immunol.* 172: 1699–1710.
26. Qi, R., D. Singh, and C. C. Kao. 2012. Proteolytic processing regulates Toll-like receptor 3 stability and endosomal localization. *J. Biol. Chem.* 287: 32617–32629.
27. Chockalingam, A., J. C. Brooks, J. L. Cameron, L. K. Blum, and C. A. Leifer. 2009. TLR9 traffics through the Golgi complex to localize to endolysosomes and respond to CpG DNA. *Immunol. Cell Biol.* 87: 209–217.
28. Bell, J. K., I. Botos, P. R. Hall, J. Askins, J. Shiloach, D. M. Segal, and D. R. Davies. 2005. The molecular structure of the Toll-like receptor 3 ligand-binding domain. *Proc. Natl. Acad. Sci. USA* 102: 10976–10980.
29. Choe, J., M. S. Kelker, and I. A. Wilson. 2005. Crystal structure of human toll-like receptor 3 (TLR3) ectodomain. *Science* 309: 581–585.
30. Ranjith-Kumar, C. T., W. Miller, J. Xiong, W. K. Russell, R. Lamb, J. Santos, K. E. Duffy, L. Cleveland, M. Park, K. Bhardwaj, et al. 2007. Biochemical and functional analyses of the human Toll-like receptor 3 ectodomain. *J. Biol. Chem.* 282: 7668–7678.
31. Botos, I., L. Liu, Y. Wang, D. M. Segal, and D. R. Davies. 2009. The toll-like receptor 3:dsRNA signaling complex. *Biochim. Biophys. Acta* 1789: 667–674.
32. Leifer, C. A., M. N. Kennedy, A. Mazzoni, C. Lee, M. J. Kruhlak, and D. M. Segal. 2004. TLR9 is localized in the endoplasmic reticulum prior to stimulation. *J. Immunol.* 173: 1179–1183.
33. Latz, E., A. Schoenemeyer, A. Visintin, K. A. Fitzgerald, B. G. Monks, C. F. Knetter, E. Lien, N. J. Nilsen, T. Espevik, and D. T. Golenbock. 2004. TLR9 signals after translocating from the ER to CpG DNA in the lysosome. *Nat. Immunol.* 5: 190–198.
34. Kasperkovitz, P. V., M. L. Cardenas, and J. M. Vyas. 2010. TLR9 is actively recruited to *Aspergillus fumigatus* phagosomes and requires the N-terminal proteolytic cleavage domain for proper intracellular trafficking. *J. Immunol.* 185: 7614–7622.
35. Sepulveda, F. E., S. Maschalidi, R. Colisson, L. Heslop, C. Ghirelli, E. Sakka, A.-M. Lennon-Duménil, S. Amigorena, L. Cabanie, and B. Manoury. 2009. Critical role for asparagine endopeptidase in endocytic Toll-like receptor signaling in dendritic cells. *Immunity* 31: 737–748.
36. Manavalan, B., S. Basith, and S. Choi. 2011. Similar structures but different roles – an updated perspective on TLR structures. *Front. Physiol.* 2: 41.
37. de Bouteiller, O., E. Merck, U. A. Hasan, S. Hubac, B. Benguigui, G. Trinchieri, E. E. Bates, and C. Caux. 2005. Recognition of double-stranded RNA by human toll-like receptor 3 and downstream receptor signaling requires multimerization and an acidic pH. *J. Biol. Chem.* 280: 38133–38145.
38. Estornes, Y., F. Toscano, F. Virard, G. Jacquemin, A. Pierrot, B. Vanbervliet, M. Bonnin, N. Lalaoui, P. Mercier-Gouy, Y. Pachéco, et al. 2012. dsRNA induces apoptosis through an atypical death complex associating TLR3 to caspase-8. *Cell Death Differ.* 19: 1482–1494.
39. Li, Y., I. C. Berke, and Y. Modis. 2012. DNA binding to proteolytically activated TLR9 is sequence-independent and enhanced by DNA curvature. *EMBO J.* 31: 919–931.

REVIEW

OncoImmunology 1:6, 1-7; September, 2012; © 2012 Landes Bioscience

TLR3/TICAM-1 signaling in tumor cell RIP3-dependent necroptosis

Tsukasa Seya,* Hiroaki Shime, Hiromi Takaki, Masahiro Azuma, Hiroyuki Oshiumi and Misako Matsumoto

Department of Microbiology and Immunology; Hokkaido University Graduate School of Medicine; Sapporo, Japan

Keywords: interferon-inducing pathway, necroptosis, RIP signaling, TLR3, TICAM-1, TLR3, TRIF

Abbreviations: CTL, cytotoxic T lymphocyte; DAI, DNA-dependent activator of IFN-regulatory factors; DAMP, damage-associated molecular pattern; HMGB1, high-mobility group box 1; HSP, heat shock protein; mDC, myeloid dendritic cell; NK, natural killer; NLR, NOD-like receptor; PAMP, pathogen- associated molecular pattern; PRR, pattern-recognition receptor; RIP, receptor-interacting protein kinase; TICAM-1, Toll-IL-1-homology domain-containing adaptor molecule 1; TLR, Toll-like receptor; TNFα, tumor necrosis factor α; TNFR1, TNFα receptor 1

The engagement of Toll-like receptor 3 (TLR3) leads to the oligomerization of the adaptor TICAM-1 (TRIF), which can induces either of three acute cellular responses, namely, cell survival coupled to Type I interferon production, or cell death, via apoptosis or necrosis. The specific response elicited by TLR3 determines the fate of affected cells, although the switching mechanism between the two cell death pathways in TLR3-stimulated cells remains molecularly unknown. Tumor necrosis factor α (TNFα)-mediated cell death can proceed via apoptosis or via a non-apoptotic pathway, termed necroptosis or programmed necrosis, which have been described in detail. Interestingly, death domain-containing kinases called receptor-interacting protein kinases (RIPs) are involved in the signaling pathways leading to these two cell death pathways. Formation of the RIP1/RIP3 complex (called necrosome) in the absence of caspase 8 activity is crucial for the induction of necroptosis in response to TNFα signaling. On the other hand, RIP1 is known to interact with the C-terminal domain of TICAM-1 and to modulate TLR3 signaling. In macrophages and perhaps tumor cell lines, RIP1/RIP3-mediated necroptotic cell death can ensue the administration of the TLR agonist polyI:C. If this involved the TLR3/TICAM-1 pathway, the innate sensing of viral dsRNA would be linked to cytopathic effects and to persistent inflammation, in turn favoring the release of damage-associated molecular patterns (DAMPs) in the microenvironment. Here, we review accumulating evidence pointing to the involvement of the TLR3/TICAM-1 axis in tumor cell necroptosis and the subsequent release of DAMPs.

Introduction

Cell death is an important process for both development and homeostasis in multicellular organisms. The mode of cell death is closely associated with other biological responses occurring within the host, including inflammation. Cell death has been categorized as apoptotic or necrotic and, until recently, apoptosis had been considered as a synonym of programmed cell death.[1] Caspases are a family of cysteine proteases that mediate apoptotic cell death in response to ligands of death receptors, including tumor necrosis factor α (TNFα), FAS ligand (FASL) and TRAIL, as well as to intracellular damage, upon the induction of pro-apoptotic BH3-only members of the Bcl-2 family. However, it is now clear that apoptosis is not the only cellular mechanism that mediates programmed cell death. Necrotic cell death, which has traditionally been viewed as a form of passive cell death, may also be regulated, and in this case has been called necroptosis or programmed necrosis.[2] Necroptosis may be induced by TNFα receptor 1 (TNFR1) agonists, but also by innate pattern-recognition receptors (PRRs) such as Toll-like receptor (TLR) 3 and TLR4.[1,4] These two TLRs can recruit the adaptor TICAM-1 (also known as TRIF), leading to Type I interferon (IFN) signaling.[3] In line with this notion, the TLR3 ligand polyI:C (a synthetic double-stranded RNA, dsRNA) can activate either apoptosis or necrosis, depending on the cell lines tested. Cell death induced by the TLR3-TICAM-1 axis may therefore be executed through two distinct subroutines.[5] The mechanisms that dictate the cellular decision to undergo apoptosis or necroptosis in response to TLR3 signaling, as well as the mechanisms that mediate the execution of necroptosis, are the subject of intense investigation.

Toll-like receptors and other PRRs harbor the ability to specifically recognize microbal molecules, known as pathogen-associated molecular patterns (PAMPs).[6] PAMPs trigger the maturation of myeloid dendritic cells (mDCs) through the activation of TLR and/or other pathways, eventually eliciting cellular immunity.[7] In mDCs, nucleic acid-recognizing TLRs (i.e., TLR3, TLR7, TLR8 and TLR9) reside in endosomes and sense their ligands only when they are internalized.[8] The uptake of DNA or RNA of microbial origin therefore allows cross-presentation to T cells and the exposure of natural killer (NK) cell-activating ligands. Besides this extrinsic maturation route, it is known that the formation of autophagosomes may deliver cytoplasmic nucleic acids of viral origin to the endosome via autophagy.[9] In either route, TLR signaling links immunological events to pathological cell death.

Recently accumulated evidence suggests that TLRs serve as receptors not only for foreign PAMPs but also for cellular

*Correspondence to: Tsukasa Seya; Email: seya-tu@pop.med.hokudai.ac.jp
Submitted: 05/28/12; Accepted: 06/22/12
http://dx.doi.org/10.4161/onci.21244

Table 1. Host response to nucleic acids and other DAMPs

PAMP/DAMP	Receptors
Microbial nucleic acids(PAMP)	
cytosolic long dsRNA	MDA5
cytosolic 5'-PPP-RNA	RIG-I
endosomal >140bp dsRNA	TLR3
nonmethylated CpG DNA	TLR9
cytosolic dsDNA	DNA sensors*
Self molecular patterns(DAMP)	
HMGB1	RAGE, TLR2/4
Uric acid	CD14, TLR2/4
HSPs	CD14, TLR2/4,**
S100 proteins	RAGE
Self nucleic acids (DAMP)	
Self DNA	DNA sensors*
Self mRNA	TLR3

*See Table 2; ** D40, CD91, Scavenger receptors etc.

Table 2. RNA·DNA recognition molecules in vertebrates

Receptors	Adaptors	Ligands	Induction of Type I IFN
		TLR family	
TLR3	TICAM-1	dsRNA, stem RNA	+
TLR7/8	MyD88	ssRNA	+
TLR22	TICAM-1	dsRNA	+
PKR	?	dsRNA	-
		RLR family	
RIG-I	MAVS	5'-PPP RNA, dsRNA	+
MDA5	MAVS	dsRNA (long)	+
		NLR family	
NALP3	ASC	dsRNA	+
NOD2	MAVS	ssRNA	+
		DDX family	
DDX1	TICAM-1	dsRNA	+
DDX21	TICAM-1	dsRNA	+
DHX36	TICAM-1	dsRNA	+
		DNA sensors	
TLR9	MyD88	CpG DNA	+
DAI	TBK1	dsDNA	+
Pol3/RIG-I	MAVS	dsDNA	+
IFI16	TBK1	dsDNA	+
DDX41	STING	dsDNA	+
DHX9	MyD88	dsDNA	+
DDX36	MyD88	dsDNA	+
ZAPS	?	dsDNA	+

constituents that are liberated from damaged or necrotic cells.[10] Thus, innate pattern-recognition is not only a mechanism for discriminating pathogens from the host, but also a means for inspecting cellular homeostasis. Molecules that, upon release from damaged/necrotic cells, activate the immune system are called damage-associated molecular patterns (DAMPs).[11] The most popular TLR adaptor MYD88 is known to contain death domains, and some reports have suggested that TLR signaling may be involved in cell death secondary to PAMP/DAMP-stimulation. Necroptotic or damaged cells may thus represent a result of TLR death signaling, and generate a functional complex consisting of sources of DAMPs as well as of the phagocytic response.[11,12]

DAMPs refer to intracellular molecules that acquire inflammation-inducing capacities when released from cells. DAMPs do not belong to the cytokine family but rather resemble PAMP in their functional properties, in particular with regard to mDC and macrophages. The functions of DAMPs may be associated with responses including regeneration and tumorigenesis. During the past 5 y, necroptotic cell death has been closely connected with innate immune responses involving pattern-sensing.[12,13] DAMPs include a large number of cytosolic or nuclear molecules (**Table 1**), as well as, surprisingly, self nucleic acids.[14] This implies that, like viral DNA and RNA, autologous nucleic acids can evoke inflammation. Here, we discuss the importance of the immune modulation induced by nucleic acids and necroptotic host cells.

Necroptosis: Programmed Necrosis Induced by TNFα

TNFα has been reported to induce two different types of cell death, apoptosis and necrosis, in a cell type-specific manner.[15,16] Through TNFR1, TNFα is implicated in NFκB activation and contributes to cell growth in many cancer cell lines. In parallel TNFα-induced hemorrhagic necrosis has been observed in several cancer cell lines, but the molecular mechanisms underlying these differential responses to TNFα remain poorly understood. Recently, several reports have suggested that the formation of a supracomplex containing the receptor-interacting protein kinase 1 (RIP1) and its homolog RIP3 (which has been named "necrosome") is responsible for the switch from apoptosis to necroptosis.[17,18] RIP1 and RIP3 can assemble only in the absence of functional caspase-8, indicating that this enzyme acts as a key protease for blocking the formation of the necrosome.[5,19] Many viral factors, as well as the genomic instability that frequently characterizes tumor cells, can compromise caspase-8 function, thereby facilitating the induction of necroptosis. Hence, TNFα can promote cell death by signaling through its receptors, including TNRF1 and downstream via RIP1/RIP3, although the output of TNFα signaling is ultimately determined by cell type.

Virus-mediated Necroptosis

It is notable that a necrotic phenotype has been observed in polyI:C-stimulated bone marrow-derived murine macrophages and other cell lines.[13] TICAM-1 and RIP3 are involved in this process, suggesting the implication of the necrosome pathway in dsRNA-mediated cell death.[12,13] It has been reported that viral

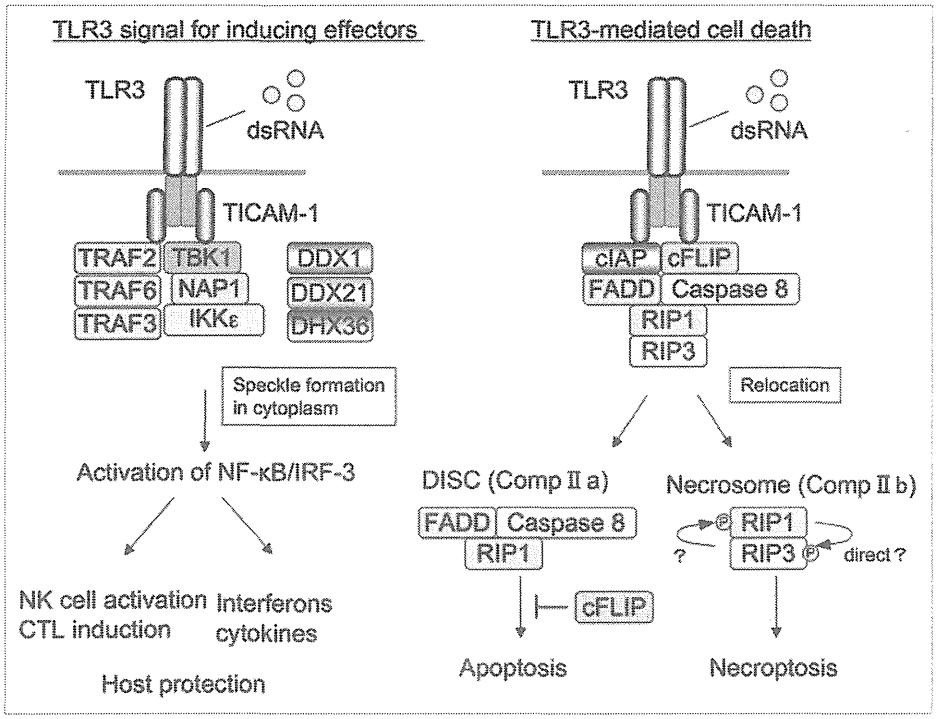

Figure 1. TLR3 signals inducing cell death or effector functions in myeloid cells. Cell survival (left panel) and cell death (right panel) signals are schematically depicted. TICAM-1 assembles in a supramolecular complex around oligomerized Toll-like receptor 3 (TLR3) in the endosome. The complex (named Speckle) then dissociates from TLR3, tranlocating to the cytoplasm. IRF-3 and NFκB are activated by Speckle, leading to their nuclear translocation and induction of Type I interferon (IFN) and inflammatory cytokines, respectively. In dendritic cells (DCs), natural killer (NK) cell-activating ligands and factors for cross-presentation are induced downstream of IRF-3/7 (left panel). In contrast, cell death signaling culminates in apoptosis and/or necrosis depending on downstream signal transducers (right panel). TLR3-dependent apoptosis has been reported in several cancer cell lines,[4] while TLR3-dependent necroptosis has been observed in mouse bone marrow-derived macrophages.[13] These events rely on RIP1/RIP3 activation, similar to those elicited upon ligation of the tumor necrosis factor α receptor 1 (TNFR1). Whether or not the translocation of the TICAM-1 complex is required for the cell death signaling, as well as the mechanisms determining either cytokine secretion or cell death, remain unknown.

dsRNA frequently induces apoptosis in infected cells, a process that in general is known as cytopathic effect.[20] TICAM-1 and RIPs, mainly RIP1, may also be involved in virus-derived necrotic cell death.[5,13] This is relatively rare compared with apoptosis since it occurs only when the viral genome encodes caspase-8 inhibitors.[19] Furthermore, this process requires viral dsRNA to be delivered from the cytosol to the endosomes (where TLR3 is situated) of infected cells. This may happen if the dsRNA is engulfed by autophagosomes, which ensure its transfer to endosomes. The possible involvement of another PRR that sense viral RNA, RIG-I/MDA5, in cell death as induced by viral infection cannot be always ruled out. TNFα can be produced downstream of the TLR3- and RIG-I-mediated RNA-sensing pathways and may induce necrotic cell death. Many RNA viruses trigger cell death,[20] but the factors determining the induction of necroptosis in virus-infected cells remain to be clarified.

DNA viruses can induce necroptosis via another mechanism, which involves the DNA-dependent activator of IFN-regulatory factors (DAI, also known as DLM-1/ZBP1).[21] DAI is a DNA sensor[22] and directly activates RIP3 in the absence of Type I IFN induction.[21] This said, the sensing of DNA in the cytoplasm of virus-infected cells is complex, and it may be that DAI is not the only molecule linked to such a necroptotic response. It is unknown whether RIP3-mediated necroptosis can be induced even if caspase-8 is blocked upon the recognition of viral DNA by DAI or via other mechanisms.[20] In fact, this type of virus-derived necrosis has been reported with DNA viruses that encode caspase inhibitors including vaccinia virus (VV), which encodes B13R/Spi2, poxvirus, encoding CrmA, the Kaposi's sarcoma-associated herpesvirus (KSHV), encoding K13 and the molluscum contagiosum virus (MCV), which encodes MC159.[20,23] Generally speaking, the mode of cell death secondary to virus infection differ as a function of viral species. The physiological role of TLR3- and DAI-mediated necroptosis should therefore be analyzed in a virus -specific fashion.

Necroptosis in Inflammation

Apoptosis plays a major role in physiological contexts, while necrosis is very common under pathological conditions.[1] Necroptosis differs from accidental necrosis in its programmed nature, and differs from apoptosis in that necroptosis often stimulates inflammation. When virus-infected cells undergo apoptosis, they are removed by phagocytosis. Viral genomes, be they either

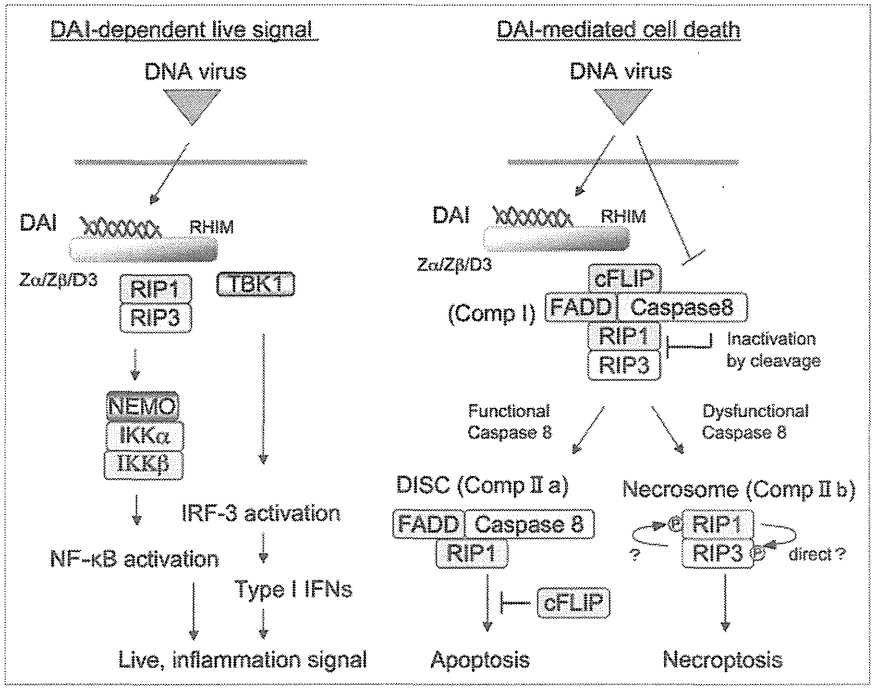

Figure 2. Necroptosis induced by the DAI pathway. Cell survival (left panel) and cell death (right panel) signals transmitted by the DNA-dependent activator of IFN-regulatory factors (DAI) are schematically depicted. Pro-survival signaling involves the activation of IRF-3 and NFκB to support antiviral responses (left panel). Type I IFNs and inflammatory cytokines are the main effectors induced by IRF-3/NFκB activation. In contrast, DAI activates RIP3 to induce necroptosis during viral infection, provided that caspases are inhibited. When viruses express caspase inhibitors, the RIP1/RIP3 necrosome plays a dominant role in the activation of cell death via necroptosis (right panel). If caspase-8 is active, RIP3 should get inactivated and apoptosis should be the dominant phenotype, though this scheme has not yet been experimentally confirmed. The mechanisms determining the choice between these two signaling pathways are unknown.

DNA- or RNA-based, are degraded in infected cells, thus being able neither to stimulate phagocytes including macrophages and DCs, nor to favor the liberation of DAMPs. In contrast, non-apoptotic cell death is accompanied by the release of DAMPs and viral products, resulting in the activation of macrophages,[13] as it occurs during chronic infection, in which viruses produce caspase inhibitors or render infected cells resistant to apoptosis.[24] A typical model of necroptosis evokes two effectors, namely, viral nucleic acids and DAMPs, to modulate immune and bystander cells of the host. In the context of necroptosis, these effectors allow for the amplification of inflammatory responses by myeloid phagocytes (mDCs and macrophages). These cells accumulate in inflammation as induced by persistent viral infection, and mediate the secondary release of cytokines and other biologically active molecules. In addition, viral factors can result in incipient inflammation, as observed in chronic infections by the hepatitis B or C virus.[24] This, in conjunction with viral nucleic acids and DAMPs, may modify the features of the infectious milieu. Further studies are needed to clarify the importance of viral nucleic acids and DAMPs in the context of virus-dependent chronic inflammation, as it may facilitate tumor progression.

Necroptosis and Oncogenesis

Accumulating evidence indicates that pro-inflammatory signals, including those following the activation of NFκB, are crucial for oncogenesis. Moreover, DAMPs have been associated with tumorigenesis as well as with antitumor immune responses.[25,26] Tumor progression is not always accompanied by viral infections, and it remains unclear whether DAMPs released from non-infected tumor cells are sufficient to support tumor growth. It has been reported that self mRNA acts as a TLR3 ligand[14] and that self DNA can stimulate host cell sensors.[22,27] Due to the uncomplete identification and functional characterization of DNA sensors and their signaling pathways, however, it is unknown whether host nucleic acids are potent inducers of inflammation as compared with viral RNA or unmethylated CpG DNA of bacterial origin. Moreover, the role of RNA sensors in the tumor microenvironment has not yet been clarified (Table 2).

DAMPs have recently been characterized at the molecular level[11] and representative DAMPs (Table 1) include HMGB1,[28] uric acid crystal,[10] S100 proteins,[29] naked actin[30,31] and heat-shock proteins (HSPs).[32] The functional features of DAMPs and the mechanisms whereby they provoke inflammation have been delineated,[11,28,29] and these studies have introduced the concept of "inflammasome" in the field of innate immunity.[33] Caspase-1 is activated upon the administration of NOD-like receptor (NLR) ligands, which include some DAMPs as well as inorganic PAMPs. Active caspase-1, together with the upregulation of the immature variants of IL-1 family proteins that ensues TLR stimulation, accelerates the robust release of IL-1β, IL-18 and IL-33.[34] There are many kinds of NLRs as well as TLRs, and the common pathways (including those centered around the adaptor ASC) can be activated by a variety of cytoplasmic DAMPs and PAMPs.[33,34] The cytoplasmic immature forms of the abovementioned cytokines are activated by limited caspase-1-mediated proteolysis, and then are secreted into the extracellular microenvironment.[34] Hence, IL-1 family proteins require two DAMPs/PAMP signals for their upregulation and activation.[35] Of note, the tumorigenic properties of asbestos and silica are in part attributable to the activation of the inflammasome, leading to the secreton of IL-1 family proteins. However, not all DAMPs operate as inflammasome activators, even in the broad sense of this term.

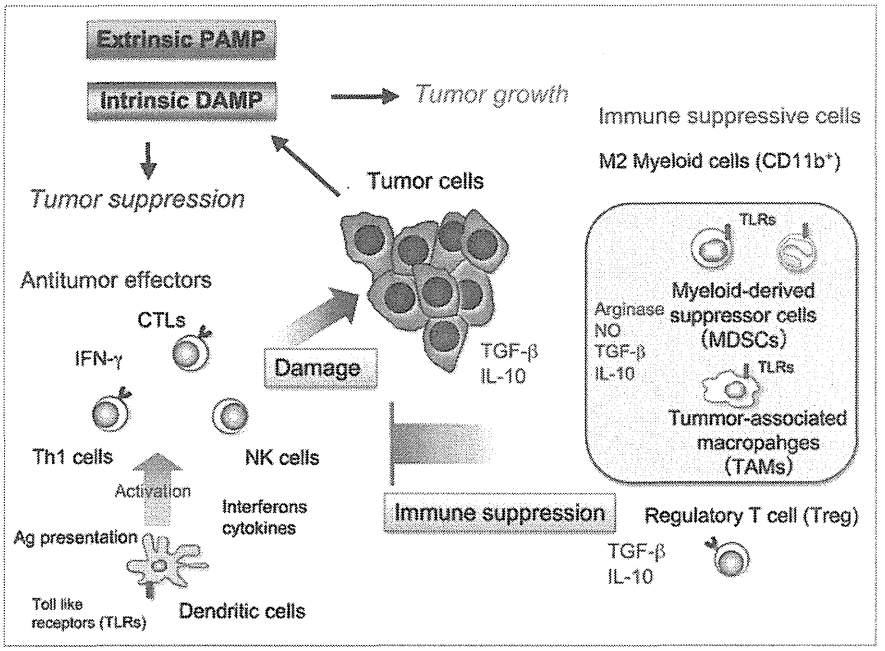

Figure 3. Inflammation provides the microenvironment for infection-related cancer. Immune cells infiltrating the tumor mass may modulate the local microenvironment upon the recognition of pathogen- or damage-associated molecular patterns (PAMP/DAMPs). Cancer cells undergoing necrosis liberate DAMPs and debris containing nucleic acids, which recruit immune cells stimulating an inflammatory response. In some cases, tumors benefit from the inflammatory response, while in other cases they regress following inflammation. The mechanisms determining this switch remain to be clarified.

Immune Response Elicited by the Phagocytosis of Dead Cells

Phagocytosis of dead cells involves not only cell clearance but also the initiation of an immune response. Dead cell antigens are rapidly presented on MHC Class II molecules after internalization by DCs, driving the recruitment and activation of various $CD4^+$ T cell subsets, including Th1, Th2, Th17 and regulatory T cells (Tregs) (**Fig. 1**). In the presence of a second co-stimulatory signal provided by TLRs, working as an adjuvant, DCs cross-present antigens on MHC Class I molecules to induce the proliferation of $CD8^+$ cytotoxic T lymphocytes (CTLs).[36] The presentation of exogenous antigens by DCs is therefore dependent on the presence of PAMPs/DAMPs.[36] Accordingly, necrotic debris appears to result in CTL cross-priming more efficiently than apoptotic bodies. Cross-presentation is enhanced by molecules such as Type I IFN and CD40, and by immune cells including $CD4^+$ T, NK and NKT cells. Hence, the use of adjuvants to affect many cell types of the immune system other than antigen-presenting cells, and a precise evaluation of the total cross-priming activity appear to be indispensable for the development of efficient adjuvant therapies.

The TLR3/TICAM-1 axis is best known as an inducer of cross-presentation in vivo.[37] The cross-presentation activity of the TLR3 ligands polyI:C and viral dsRNA was first described by Schulz et al. in 2005.[38] While the potency of polyI:C as an adjuvant has been reported by Steinman and colleagues,[37,39] the precise identity of the DAMPs participating in cross-presentation and possessing latent cross-priming (CTL-inducing) capacities has not yet been determined.

It is known that phagocytosis induces functional changes in mDCs and macrophages (**Fig. 2**): phagocytes are skewed toward a regulatory phenotype accompanied by the production of IL-10 and TGFβ during the phagocytosis of apoptotic cell debris, even in the presence of PAMP.[40,41] This suggests that material that cannot be taken up exerts different effects on mDCs than internalizable material during their phagocytic interactions. Phagocytes undergo cytoskeletal rearrangement when they take up cell debris, involving cell adhesion molecules that accelerate the interaction between the phagocyte membrane and cell debris. The opsonization of dead cells further enhances phagocytosis as well as the induction of an immune outcome.[42] Complement-mediated opsonization of dead cells strongly alters the functional properties of mDCs and macrophages.[43] Yet, it has been impossible to discriminate apoptotic and necroptotic cells based on this.[44] Thus, the mechanisms whereby necroptotic cells initiate an immune response upon phagocytosis by mDCs and macrophages, compared with apoptotic cells, remain largely uncharacterized. Elucidating the role of necroptotic cells and DAMPs as adjuvants for NK-cell activation and antigen presentation is highly relevant for antitumor therapy. Since the phagocytosis of dead cells by mDCs usually leads to the generation of tolerogenic mDCs, additional adjuvants appear to be required for mDCs to present tumor antigens in an immunogenic fashion, leading to the induction of an effective immune response against cancer.

Termination of Inflammation

Inflammation often drives tissue repair and regeneration, and the microenvironment formed during inflammation serves a basis for assembling cells that initiate tissue development and reorganization (**Fig. 3**). The pro-inflammatory microenvironment facilitates cell growth as well as genome instability, thus being prone to the accumulation of cells with multiple mutations. Furthermore, incipient inflammation compromises the immune system so that the abnormal proliferation of transformed cells is tolerated. Thus, malignant cells build up a tissue that involves tumor-associated macrophages serving a scaffold for invasion and metastasis.[45] In this context, a region harboring DAMP-mediated persistent inflammation provides a perfect nest for tumor progression (**Fig. 3**). Therapeutics for suppressing inflammation, such as aspirin, may constitute an immune therapy irrespective of the presence of infection.[46] We surmise that two types of inflammation exist, namely tumor-supporting and tumor-suppressing, implying that inflammation is a complex phenomenon consisting of multiple distinct aspects. We have shown that some adjuvants can induce tumor-suppressing inflammation, thereby limiting tumor proliferation by DAMPs.[47] The adjuvant-induced switch of cell death/inflammation signals to an antitumor outcome is an intriguing approach for cancer therapy, particularly in view of the fact that the mechanisms of adjuvant signaling are being increasingly characterized at the molecular level.[48,49] The clarification of the role of adjuvant signaling in compromising tumor progression will lead to the discovery of non-toxic synthetic tumor-regressing molecules with potential as novel anticancer therapeutics.[50]

Acknowledgments

We thank Drs. H. H. Aly, R. Takemura, A. Maruyama, Sayuri Yamazaki and J. Kasamatsu in our laboratory for their fruitful discussions. This work was supported in part by Grants-in-Aid from the Ministry of Education, Science and Culture (Specified Project for Advanced Research, MEXT) and the Ministry of Health, Labor and Welfare of Japan and by the Takeda and the Waxmann Foundations. Financial supports by a MEXT Grant-in-Project 'the Carcinogenic Spiral', 'the National Cancer Center Research and Development Fund (23-A-44)' and the Japan Initiative for Global Research Network on Infectious Diseases (J-GRID) are gratefully acknowledged.

References

1. Kroemer G, Galluzzi L, Vandenabeele P, Abrams J, Alnemri ES, Baehrecke EH, et al.; Nomenclature Committee on Cell Death 2009. Classification of cell death: recommendations of the Nomenclature Committee on Cell Death 2009. Cell Death Differ 2009; 16:3-11; PMID:18846107; http://dx.doi.org/10.1038/cdd.2008.150.
2. Tait SW, Green DR. Caspase-independent cell death: leaving the set without the final cut. Oncogene 2008; 27:6452-61; PMID:18955972; http://dx.doi.org/10.1038/onc.2008.311.
3. Oshiumi H, Sasai M, Shida K, Fujita T, Matsumoto M, Seya T. TIR-containing adapter molecule (TICAM)-2, a bridging adapter recruiting to toll-like receptor 4 TICAM-1 that induces interferon-beta. J Biol Chem 2003; 278:49751-62; PMID:14519765; http://dx.doi.org/10.1074/jbc.M305820200.
4. Ermolaeva MA, Michallet MC, Papadopoulou N, Utermöhlen O, Kranidioti K, Kollias G, et al. Function of TRADD in tumor necrosis factor receptor 1 signaling and in TRIF-dependent inflammatory responses. Nat Immunol 2008; 9:1037-46; PMID:18641654; http://dx.doi.org/10.1038/ni.1638.
5. Feoktistova M, Geserick P, Kellert B, Dimitrova DP, Langlais C, Hupe M, et al. cIAPs block Ripoptosome formation, a RIP1/caspase-8 containing intracellular cell death complex differentially regulated by cFLIP isoforms. Mol Cell 2011; 43:449-63; PMID:21737330; http://dx.doi.org/10.1016/j.molcel.2011.06.011.
6. Medzhitov R, Janeway CA Jr. Innate immunity: the virtues of a nonclonal system of recognition. Cell 1997; 91:295-8; PMID:9363937; http://dx.doi.org/10.1016/S0092-8674(00)80412-2.
7. Iwasaki A, Medzhitov R. Regulation of adaptive immunity by the innate immune system. Science 2010; 327:291-5; PMID:20075244; http://dx.doi.org/10.1126/science.1183021.
8. Kawai T, Akira S. Toll-like receptor and RIG-I-like receptor signaling. Ann N Y Acad Sci 2008; 1143:1-20; PMID:19076341; http://dx.doi.org/10.1196/annals.1443.020.
9. Morris S, Swanson MS, Lieberman A, Reed M, Yue Z, Lindell DM, et al. Autophagy-mediated dendritic cell activation is essential for innate cytokine production and APC function with respiratory syncytial virus responses. J Immunol 2011; 187:3953-61; PMID:21911604; http://dx.doi.org/10.4049/jimmunol.1100524.
10. Chen CJ, Kono H, Golenbock D, Reed G, Akira S, Rock KL. Identification of a key pathway required for the sterile inflammatory response triggered by dying cells. Nat Med 2007; 13:851-6; PMID:17572686; http://dx.doi.org/10.1038/nm1603.
11. Kono H, Rock KL. How dying cells alert the immune system to danger. Nat Rev Immunol 2008; 8:279-89; PMID:18340345; http://dx.doi.org/10.1038/nri2215.
12. Cavassani KA, Ishii M, Wen H, Schaller MA, Lincoln PM, Lukacs NW, et al. TLR3 is an endogenous sensor of tissue necrosis during acute inflammatory events. J Exp Med 2008; 205:2609-21; PMID:18838547; http://dx.doi.org/10.1084/jem.20081370.
13. He S, Liang Y, Shao F, Wang X. Toll-like receptors activate programmed necrosis in macrophages through a receptor-interacting kinase-3-mediated pathway. Proc Natl Acad Sci U S A 2011; 108:20054-9; PMID:22123964; http://dx.doi.org/10.1073/pnas.1116302108.
14. Karikó K, Ni H, Capodici J, Lamphier M, Weissman D. mRNA is an endogenous ligand for Toll-like receptor 3. J Biol Chem 2004; 279:12542-50; PMID:14729660; http://dx.doi.org/10.1074/jbc.M310175200.
15. Zhang DW, Shao J, Lin J, Zhang N, Lu BJ, Lin SC, et al. RIP3, an energy metabolism regulator that switches TNF-induced cell death from apoptosis to necrosis. Science 2009; 325:332-6; PMID:19498109; http://dx.doi.org/10.1126/science.1172308.
16. Vandenabeele P, Declercq W, Van Herreweghe F, Vanden Berghe T. The role of the kinases RIP1 and RIP3 in TNF-induced necrosis. Sci Signal 2010; 3:re4; PMID:20354226; http://dx.doi.org/10.1126/scisignal.3115re4.
17. He S, Wang L, Miao L, Wang T, Du F, Zhao L, et al. Receptor interacting protein kinase-3 determines cellular necrotic response to TNF-alpha. Cell 2009; 137:1100-11; PMID:19524512; http://dx.doi.org/10.1016/j.cell.2009.05.021.
18. Cho YS, Challa S, Moquin D, Genga R, Ray TD, Guildford M, et al. Phosphorylation-driven assembly of the RIP1-RIP3 complex regulates programmed necrosis and virus-induced inflammation. Cell 2009; 137:1112-23; PMID:19524513; http://dx.doi.org/10.1016/j.cell.2009.05.037.
19. Kaiser WJ, Upton JW, Long AB, Livingston-Rosanoff D, Daley-Bauer LP, Hakem R, et al. RIP3 mediates the embryonic lethality of caspase-8-deficient mice. Nature 2011; 471:368-72; PMID:21368762; http://dx.doi.org/10.1038/nature09857.
20. Galluzzi L, Brenner C, Morselli E, Touat Z, Kroemer G. Viral control of mitochondrial apoptosis. PLoS Pathog 2008; 4:e1000018; PMID:18516228; http://dx.doi.org/10.1371/journal.ppat.1000018.
21. Upton JW, Kaiser WJ, Mocarski ES. DAI/ZBP1/DLM-1 complexes with RIP3 to mediate virus-induced programmed necrosis that is targeted by murine cytomegalovirus vIRA. Cell Host Microbe 2012; 11:290-7; PMID:22423968; http://dx.doi.org/10.1016/j.chom.2012.01.016.
22. Takaoka A, Wang Z, Choi MK, Yanai H, Negishi H, Ban T, et al. DAI (DLM-1/ZBP1) is a cytosolic DNA sensor and an activator of innate immune response. Nature 2007; 448:501-5; PMID:17618271; http://dx.doi.org/10.1038/nature06013.
23. Shisler JL, Moss B. Immunology 102 at poxvirus U: avoiding apoptosis. Semin Immunol 2001; 13:67-72; PMID:11289801; http://dx.doi.org/10.1006/smim.2000.0297.
24. Saeed M, Shiina M, Date T, Akazawa D, Watanabe N, Murayama A, et al. In vivo adaptation of hepatitis C virus in chimpanzees for efficient virus production and evasion of apoptosis. Hepatology 2011; 54:425-33; PMID:21538444; http://dx.doi.org/10.1002/hep.24399.
25. Salaun B, Romero P, Lebecque S. Toll-like receptors' two-edged sword: when immunity meets apoptosis. Eur J Immunol 2007; 37:3311-8; PMID:18034428; http://dx.doi.org/10.1002/eji.200737744.
26. Piccinini AM, Midwood KS. DAMPening inflammation by modulating TLR signalling. Mediators Inflamm. 2010; pii: 672395.

27. Ishii KJ, Kawagoe T, Koyama S, Matsui K, Kumar H, Kawai T, et al. TANK-binding kinase-1 delineates innate and adaptive immune responses to DNA vaccines. Nature 2008; 451:725-9; PMID:18256672; http://dx.doi.org/10.1038/nature06537.
28. Yanai H, Ban T, Wang Z, Choi MK, Kawamura T, Negishi H, et al. HMGB proteins function as universal sentinels for nucleic-acid-mediated innate immune responses. Nature 2009; 462:99-103; PMID:19890330; http://dx.doi.org/10.1038/nature08512.
29. Hiratsuka S, Watanabe A, Sakurai Y, Akashi-Takamura S, Ishibashi S, Miyake K, et al. The S100A8-serum amyloid A3-TLR4 paracrine cascade establishes a pre-metastatic phase. Nat Cell Biol 2008; 10:1349-55; PMID:18820689; http://dx.doi.org/10.1038/ncb1794.
30. Ahrens S, Zelenay S, Sancho D, Han P, Kjær S, Feest C, et al. F-actin is an evolutionarily conserved damage-associated molecular pattern recognized by DNGR-1, a receptor for dead cells. Immunity 2012; 36:635-45; PMID:22483800; http://dx.doi.org/10.1016/j.immuni.2012.03.008.
31. Zhang JG, Czabotar PE, Policheni AN, Caminschi I, Wan SS, Kitsoulis S, et al. The dendritic cell receptor Clec9A binds damaged cells via exposed actin filaments. Immunity 2012; 36:646-57; PMID:22483802; http://dx.doi.org/10.1016/j.immuni.2012.03.009.
32. Tsan MF, Gao B. Heat shock proteins and immune system. J Leukoc Biol 2009; 85:905-10; PMID:19276179; http://dx.doi.org/10.1189/jlb.0109005.
33. Pedra JH, Cassel SL, Sutterwala FS. Sensing pathogens and danger signals by the inflammasome. Curr Opin Immunol 2009; 21:10-6; PMID:19223160; http://dx.doi.org/10.1016/j.coi.2009.01.006.
34. Cassel SL, Joly S, Sutterwala FS. The NLRP3 inflammasome: a sensor of immune danger signals. Semin Immunol 2009; 21:194-8; PMID:19501527; http://dx.doi.org/10.1016/j.smim.2009.05.002.
35. Yu HB, Finlay BB. The caspase-1 inflammasome: a pilot of innate immune responses. Cell Host Microbe 2008; 4:198-208; PMID:18779046; http://dx.doi.org/10.1016/j.chom.2008.08.007.
36. Seya T, Shime H, Ebihara T, Oshiumi H, Matsumoto M. Pattern recognition receptors of innate immunity and their application to tumor immunotherapy. Cancer Sci 2010; 101:313-20; PMID:20059475; http://dx.doi.org/10.1111/j.1349-7006.2009.01442.x.
37. Caskey M, Lefebvre F, Filali-Mouhim A, Cameron MJ, Goulet JP, Haddad EK, et al. Synthetic double-stranded RNA induces innate immune responses similar to a live viral vaccine in humans. J Exp Med 2011; 208:2357-66; PMID:22065672; http://dx.doi.org/10.1084/jem.20111171.
38. Schulz O, Diebold SS, Chen M, Näslund TI, Nolte MA, Alexopoulou L, et al. Toll-like receptor 3 promotes cross-priming to virus-infected cells. Nature 2005; 433:887-92; PMID:15711573; http://dx.doi.org/10.1038/nature03326.
39. Longhi MP, Trumpfheller C, Idoyaga J, Caskey M, Matos I, Kluger C, et al. Dendritic cells require a systemic type I interferon response to mature and induce CD4+ Th1 immunity with poly IC as adjuvant. J Exp Med 2009; 206:1589-602; PMID:19564349; http://dx.doi.org/10.1084/jem.20090247.
40. Chung EY, Kim SJ, Ma XJ. Regulation of cytokine production during phagocytosis of apoptotic cells. Cell Res 2006; 16:154-61; PMID:16474428; http://dx.doi.org/10.1038/sj.cr.7310021.
41. Zhang Y, Kim HJ, Yamamoto S, Kang X, Ma X. Regulation of interleukin-10 gene expression in macrophages engulfing apoptotic cells. J Interferon Cytokine Res 2010; 30:113-22; PMID:20187777; http://dx.doi.org/10.1089/jir.2010.0004.
42. Aderem A, Underhill DM. Mechanisms of phagocytosis in macrophages. Annu Rev Immunol 1999; 17:593-623; PMID:10358769; http://dx.doi.org/10.1146/annurev.immunol.17.1.593.
43. Ricklin D, Hajishengallis G, Yang K, Lambris JD. Complement: a key system for immune surveillance and homeostasis. Nat Immunol 2010; 11:785-97; PMID:20720586; http://dx.doi.org/10.1038/ni.1923.
44. Wakasa K, Shime H, Kurita-Taniguchi M, Matsumoto M, Imamura M, Seya T. Development of monoclonal antibodies that specifically interact with necrotic lymphoma cells. Microbiol Immunol 2011; 55:373-7; PMID:21517948; http://dx.doi.org/10.1111/j.1348-0421.2011.00319.x.
45. Mantovani A. La mala educación of tumor-associated macrophages: Diverse pathways and new players. Cancer Cell 2010; 17:111-2; PMID:20159603; http://dx.doi.org/10.1016/j.ccr.2010.01.019.
46. Chan AT, Ogino S, Fuchs CS. Aspirin and the risk of colorectal cancer in relation to the expression of COX-2. N Engl J Med 2007; 356:2131-42; PMID:17522398; http://dx.doi.org/10.1056/NEJMoa067208.
47. Shime H, Matsumoto M, Oshiumi H, Tanaka S, Nakane A, Iwakura Y, et al. Toll-like receptor 3 signaling converts tumor-supporting myeloid cells to tumoricidal effectors. Proc Natl Acad Sci U S A 2012; 109:2066-71; PMID:22308357; http://dx.doi.org/10.1073/pnas.1113099109.
48. Ishii KJ, Akira S. Toll or toll-free adjuvant path toward the optimal vaccine development. J Clin Immunol 2007; 27:363-71; PMID:17370119; http://dx.doi.org/10.1007/s10875-007-9087-x.
49. Seya T, Matsumoto M. The extrinsic RNA-sensing pathway for adjuvant immunotherapy of cancer. Cancer Immunol Immunother 2009; 58:1175-84; PMID:19184005; http://dx.doi.org/10.1007/s00262-008-0652-9.
50. Galluzzi L, Vacchelli E, Eggermont A, Fridman WH, Galon J, Sautes-Fridman C, et al. Trial Watch: Experimental Toll-like receptor agonists for cancer therapy. OncoImmunol. 2012; In press.

OncoImmunology 1:6, 1-2; September, 2012; © 2012 Landes Bioscience

TAMable tumor-associated macrophages in response to innate RNA sensing

Tsukasa Seya,* Hiroaki Shime and Misako Matsumoto

Department of Microbiology and Immunology; Graduate School of Medicine; Hokkaido University; Sapporo, Japan

Key words: TLR3, TICAM-1, tumor-infiltrating macrophages, polyI:C, immunotherapy

Antitumor effect of PolyI:C (a viral dsRNA analog) has been attributed to dendritic cell (DC)-maturation activity, that drives antitumor NK cells, DC cross-presentation, cytotoxic T lymphocytes and many IFN-inducible genes. According to a recent paper, tumor-infiltrating M2 macrophages are found to become an additional antitumor effector through polyI:C response.

Interferon (IFN), now categorized as type I, was discovered by Isaacs and Lindeman in 1957. Soon after their discovery, it was expected to be a fascinating medicine opposing to virus infection and cancer development. Type I IFN inducing activity was assigned to the signature of double-stranded RNA generated from viruses, and its synthetic analog, polyI:C, was confirmed to serve as an effective inducer of type I IFN. Talmadge et al. showed that polyI:C mixed with polyL Lysine and methylcellulose (polyI:CLC) effected dramatic regression of syngenic implant tumors in mice. They suggested this reagent might be applied to antitumor therapy. In line with these reports, there have been many reports indicating that spontaneous tumor regression sometimes occurrs in cancer patients when they are exposed to viruses or viral vectors.

PolyI:C induces type I IFN and inflammatory cytokines. In addition, it may contribute to raising cellular immunity. According to recent progress in pattern recognition of innate immunity, polyI:C is a ligand for multiple receptors, including PKR, RIG-I, MDA5 and TLR3.[2] Virus replication usually amplifies dsRNA production inside the cytoplasm of affected cells and stimulates the cytoplasmic RNA sensors. In contrast, TLR3 is activated when dsRNA generated in infected cells is released and internalized into the endosome of bystander phagocytes,[2] such as dendritic cells (DC) and macrophages. dsRNA is delivered through a unique pathway involving Raftlin,[3] then the endosomal TLR3 passes the signal to the adaptor TICAM-1.[2] The multiple functionality of polyI:C may reflect its divergent receptor usage, and knockout mouse (KO) studies have therefore been indispensable for determination of the role of each receptor in antitumor immunity.

In mouse models, growth retardation of syngenic implanted tumor has been reportedly observed by administration of polyI:C, which is now attributable to liberated type I IFN and maturation of DC, that drives NK and killer T cells.[4,5] The mechanisms whereby these effector cells are introduced by dsRNA are being elucidated on a molecular level: the TLR3/TICAM-1 pathway for dsRNA recognition in DC is involved in effector driving. In a recent paper, Shime et al. additionally identified the third antitumor effector induced by ip polyI:C administration.[6] PolyI:C acted on tumor-infiltrating macrophages and induced tumor growth retardation in some tumor species. Administration of polyI:C rapidly (< 12 h) led to tumor hemorrhagic necrosis followed by tumor regression. The results appear to resemble an earlier report by Old's group on the TNFα-mediated fibrosarcoma regression.[7] In fact, TNFα participated in hemorrhagic necrosis in this case also. Shime et al. applied KO mice models for analyzing the signaling pathway by which the polyI:C-derived tumor regression occurs. Ultimately, their conclusion was that tumor-infiltrating macrophages (Mf) characterized by $CD11b^{+}$/$F4/80^{+}$/$Gr\text{-}1^{low}$ markers with sustaining tumor-supporting phenotype, M2, serves as a target for polyI:C and changes their properties to antitumor, M1-like, behaving like a tumoricidal effector. In these Mf, TLR3/TICAM-1 pathway, but not the IPS-1 pathway, is also mandatory for TNFα production and tumor regression. Indeed, the marker profile of the Mf was similar to those reported as M2 Mf or tumor-associated Mf (TAM). It is notable that they have high expression levels of TLR3. Hence, the polyI:C tumor growth retardation is mechanically multifarious and involves TNFα hemorrhagic necrosis.

TLR3 is highly expressed in $CD8^{+}$ splenic DC and $CD103^{+}$ non-lymphoid DC in mice,[8] and they are strong inducers for cross-priming of CD8 T cells,[5,8] namely cytotoxic T lymphocytes (CTL). TLR3-positive bone marrow-derived DC also reportedly induce type I IFN and potent antitumor NK cell activity.[4] Thus, polyI:C functions through $TLR3^{+}$ myeloid cells to facilitates antitumor cellular immunity encompassing at least three distinct routes, NK cell activation, CTL proliferation and conversion of TAM to an tumoricidal effector (**Fig. 1**). Hence,

*Correspondence to: Tsukasa Seya; Email: seya-tu@pop.med.hokudai.ac.jp
Submitted: 02/27/12; Revised: 03/02/12; Accepted: 03/02/12
http://dx.doi.org/

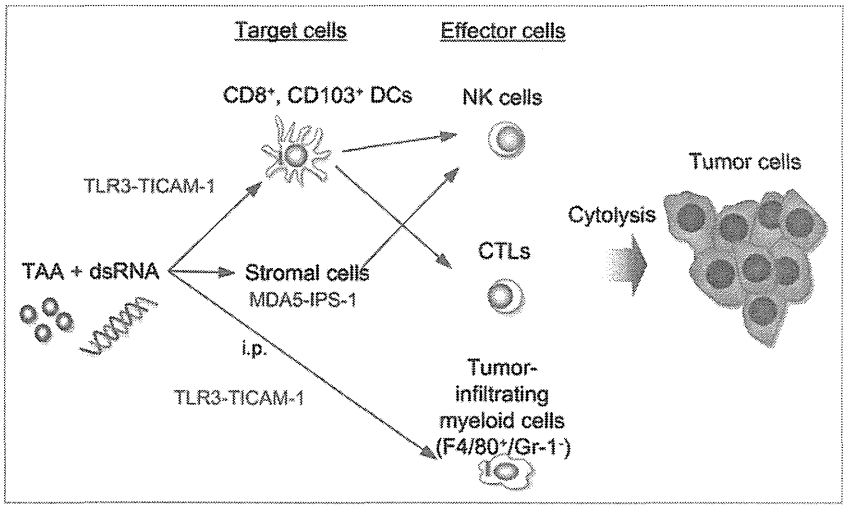

Figure 1. PolyI:C induces three antitumor effectors via different routes. Antitumor activity of polyI:C against tumor cells are assessed in mouse tumor-implant models. A unique point in this review is the third pathway where tumor-infiltrating myeloid cells are involved, effectively damages Lewis Lung carcinoma cells. This tumoricidal activity is mediated by the TICAM-1 pathway in the myeloid cells, and attributed to TNFα. Although polyI:C is i.p. administered, it acts on tumor-infiltrating Mf and converts them to antitumor effectors.

the Janeway/Medzhitov concept[9] may be adaptable to tumor immunology that pattern recognition receptor (PRR) stimulation by a specific ligand triggers innate immune response and facilitates establishment of the cellular immune system.

A tantalizing reagent for successful peptide vaccine therapy against cancer using tumor-associated antigens (TAA) with CD4/CD8 epitopes is adjuvant. Nevertheless, polyI:C therapeutic use has been very restricted in patients. This is because polyI:C has severe side effects, enterocolitis, arthralgia, fever, erythema and sometimes life-threatening hypotonic shock, which have prevented the clinical use of this dsRNA analog. However, a recent study reported that polyI:CLC is applicable to humans, although robust erythema and cytokine upregulation in serum are usually accompanied as side effects with expected therapeutic potential.[10] Dr. Steinman, having won the Nobel prize, proposed a polyI:C/TAA therapy for cancer patients if the TAA is identified in each case of the patients. Shime's data confirmed this issue and further clarified the importance of the TICAM-1 pathway in triggering induction of antitumor Mf in addtion to NK cells and CTL.[6] These sequential studies, together with the direct apoptotic effect of polyI:C on tumor cells, reinforce the need to establish a safer RNA derivative for human immunotherapy in the future.

References

1. Talmadge JE, Adams J, Phillips H, Collins M, Lenz B, Schneider M, et al. Immunomodulatory effects in mice of polyinosinic-polycytidylic acid complexed with poly-L-lysine and carboxymethylcellulose. Cancer Res 1985; 45:1058-65; PMID:3155990.
2. Matsumoto M, Oshiumi H, Seya T. Antiviral responses induced by the TLR3 pathway. Rev Med Virol 2011; 21:67-77; PMID:21312311; http://dx.doi.org/10.1002/rmv.680.
3. Watanabe A, Tatematsu M, Saeki K, Shibata S, Shime H, Yoshimura A, et al. Raftlin is involved in the nucleocapture complex to induce poly(I:C)-mediated TLR3 activation. J Biol Chem 2011; 286:10702-11; PMID:21266579; http://dx.doi.org/10.1074/jbc.M110.185793.
4. Ebihara T, Azuma M, Oshiumi H, Kasamatsu J, Iwabuchi K, Matsumoto K, et al. Identification of a polyI:C-inducible membrane protein that participates in dendritic cell-mediated natural killer cell activation. J Exp Med 2010; 207:2675-87; PMID:21059856; http://dx.doi.org/10.1084/jem.20091573.
5. Azuma M, Ebihara T, Oshiumi H, Matsumoto M, Seya T. Cross-priming for antitumor CTL induced by soluble Ag + polyI:C depends on the TICAM-1 pathway in mouse CD11c+/CD8α+ dendritic cells. OncoImmunol 2012; In press.
6. Shime H, Matsumoto M, Oshiumi H, Tanaka S, Nakane A, Iwakura Y, et al. Toll-like receptor 3 signaling converts tumor-supporting myeloid cells to tumoricidal effectors. Proc Natl Acad Sci USA 2012; 109:2066-71; PMID:22308357; http://dx.doi.org/10.1073/pnas.1113099109.
7. Carswell EA, Old LJ, Kassel RL, Green S, Fiore N, Williamson B. An endotoxin-induced serum factor that causes necrosis of tumors. Proc Natl Acad Sci USA 1975; 72:3666-70; PMID:1103152; http://dx.doi.org/10.1073/pnas.72.9.3666.
8. Jelinek I, Leonard JN, Price GE, Brown KN, Meyer-Manlapat A, Goldsmith PK, et al. TLR3-specific double-stranded RNA oligonucleotide adjuvants induce dendritic cell cross-presentation, CTL responses and antiviral protection. J Immunol 2011; 186:2422-9; PMID:21242525; http://dx.doi.org/10.4049/jimmunol.1002845.
9. Medzhitov R, Preston-Hurlburt P, Janeway CA Jr. A human homologue of the Drosophila Toll protein signals activation of adaptive immunity. Nature 1997; 388:394-7; PMID:9237759; http://dx.doi.org/10.1038/41131.
10. Caskey M, Lefebvre F, Filali-Mouhim A, Cameron MJ, Goulet JP, Haddad EK, et al. Synthetic double-stranded RNA induces innate immune responses similar to a live viral vaccine in humans. J Exp Med 2011; 208:2357-66; PMID:22065672; http://dx.doi.org/10.1084/jem.20111171.

J. Biochem. 2012;151(1):5–11 doi:10.1093/jb/mvr111

JB THE JOURNAL OF BIOCHEMISTRY

JB Review

Ubiquitin-mediated modulation of the cytoplasmic viral RNA sensor RIG-I

Received July 11, 2011; accepted August 17, 2011; published online September 2, 2011

Hiroyuki Oshiumi*, Misako Matsumoto and Tsukasa Seya

Department of Microbiology and Immunology, Graduate School of Medicine, Hokkaido University, Kita-15, Nishi-7, Kita-ku Sapporo 060-8638, Japan

*To whom correspondence should be addressed.
Tel: +81-11-706-5056, Fax: +81-11-706-7866,
E-mail: oshiumi@med.hokudai.ac.jp

RIG-I-like receptors, including RIG-I, MDA5 and LGP2, recognize cytoplasmic viral RNA. The RIG-I protein consists of N-terminal CARDs, central RNA helicase and C-terminal domains. RIG-I activation is regulated by ubiquitination. Three ubiquitin ligases target the RIG-I protein. TRIM25 and Riplet ubiquitin ligases are positive regulators of RIG-I and deliver the K63-linked polyubiquitin moiety to RIG-I CARDs and the C-terminal domain. RNF125, another ubiquitin ligase, is a negative regulator of RIG-I and mediates K48-linked polyubiquitination of RIG-I, leading to the degradation of the RIG-I protein by proteasomes. The K63-linked polyubiquitin chains of RIG-I are removed by a deubiquitin enzyme, CYLD. Thus, CYLD is a negative regulator of RIG-I. Furthermore, TRIM25 itself is regulated by ubiquitination. HOIP and HOIL proteins are ubiquitin ligases and are also known as linear ubiquitin assembly complexes (LUBACs). The TRIM25 protein is ubiquitinated by LUBAC and then degraded by proteasomes. The splice variant of RIG-I encodes a protein that lacks the first CARD of RIG-I, and the variant RIG-I protein is not ubiquitinated by TRIM25. Therefore, ubiquitin is the key regulator of the cytoplasmic viral RNA sensor RIG-I.

Keywords: RIG-I/type I interferon/ubiquitin/virus.

Abbreviations: CARD, caspase activation and recruitment domain; CTD, C-terminal domain; dsRNA, double-stranded RNA; RLR, RIG-I-like receptor; pDC, plasmacytoid dendritic cell; cDC, conventional dendritic cell; MEF, mouse embryonic fibroblast cell; BM, bone-marrow; Mf, macrophage; IFN, interferon; ISG, interferon-stimulated gene; TRIM, tripartite motif; RNF, RING finger.

Recognition of viral RNA

Type I interferons (IFNs) are inflammatory cytokines that possess strong anti-viral activity. During viral infection, type I IFNs are produced from dendritic cells (DC), macrophages (Mf) and fibroblast cells (Fig. 1A). Viral RNA is mainly recognized by Toll-like receptors (TLRs) and RIG-I-like receptors (RLRs). TLRs are type I transmembrane proteins. TLR3, 7 and 8, which are members of the TLR family, are localized to endosomes, and are responsible for the recognition of viral RNA (*1*). RLRs are DExD/H box RNA helicases and recognize viral RNA in the cytoplasmic region (Fig. 1B). There are three members of the RLR family: RIG-I, MDA5 and LGP2. RIG-I has the ability to recognize various types of viruses, and MDA5 mainly recognizes picornaviruses (*2*). LGP2 promotes RIG-I and MDA5-mediated signalling (*3*).

A cytoplasmic sensor for the detection of viral RNA

RIG-I, a cytoplasmic sensor for viral RNA, is induced by viral infection, polyIC and type I IFN stimulation (*4*). This protein is composed of two N-terminal caspase recruitment domains (CARDs), a central DExD/H box helicase/ATPase domain and a C-terminal regulatory domain (CTD) (Fig. 2). N-terminal CARDs are responsible for the binding to the adaptor molecule IPS-1/MAVS/VISA/Cardif, which is located on the outer membrane of the mitochondria (*5–8*). In the absence of viral RNA, RIG-I CTD represses the interaction between RIG-I CARDs and IPS-1 CARD (*9*). RIG-I CTD recognizes the 5′ triphosphate of short double-stranded RNA, leading to multimerization of RIG-I and IPS-1 (*10–13*). IPS-1 triggers signaling to induce type I IFN and other inflammatory cytokines through STING (also called MITA) protein, which is localized to the endoplasmic reticulum or the mitochondria (*14–17*). STING then activates transcription factors, such as IRF-3, IRF-7 and NF-κB (*15, 18*).

Knockout of RIG-I abrogates the production of type I IFNs and inflammatory cytokines from mouse embryonic fibroblasts (MEFs), conventional DC and Mfs in response to viral infections, including infections caused by vesicular stomatitis virus (VSV), Sendai virus (SeV), influenza A virus, Newcastle disease virus, hepatitis C virus and Japanese encephalitis virus (*2, 19*). However, RIG-I is not necessary for the production of type I IFNs by plasmacytoid dendritic cells (pDCs), which are strong inducers of type I IFNs *in vivo* (*19*). In pDCs, TLR7 is responsible for the detection of viral RNA (*20*). In addition, knockout of IPS-1 and STING inhibits the production of type I IFNs from MEFs, Mfs and cDCs, but not from pDCs (*15–18*). Once type I IFNs are produced from these cells, IFN production is secondly amplified via the IFNAR (*21*). The deficiency of the RIG-I-dependent pathway causes a reduction in early type I IFN production *in vivo* but shows only a marginal effect on late type I IFN production (*15–18*). Knockout of RIG-I increases the